Mon. Not. R. Astron. Soc. **349,** 1193–1210 (2004) doi:10.1111/j.1365-2966.2004.07626.x

Chandra observations of five ultraluminous X-ray sources in nearby galaxies

T. P. Roberts,[1]★ R. S. Warwick,[1] M. J. Ward[1] and M. R. Goad[2]

[1]*X-ray and Observational Astronomy Group, Department of Physics & Astronomy, University of Leicester, University Road, Leicester LE1 7RH*
[2]*Department of Physics & Astronomy, University of Southampton, Highfield, Southampton SO17 1BJ*

Accepted 2004 January 13. Received 2003 December 17; in original form 2003 May 19

ABSTRACT

We report the results of a programme of dual-epoch *Chandra* ACIS-S observations of five ultraluminous X-ray sources (ULXs) in nearby spiral galaxies. All five ULXs are detected as unresolved, point-like X-ray sources by *Chandra*, though two have faded below the 10^{39} erg s^{-1} luminosity threshold used to first designate these sources as ULXs. Using this same criterion, we detect three further ULXs within the imaged regions of the galaxies. The ULXs appear to be related to the star-forming regions of the galaxies, indicating that even in normal spiral galaxies the ULX population is predominantly associated with young stellar populations. A detailed study of the *Chandra* ACIS-S spectra of six of the ULXs shows that five are better described by a power-law continuum than a multicolour disc blackbody model, though there is evidence for additional very soft components to two of the power-law continua. The measured photon indices in four out of five cases are consistent with the low/hard state in black hole binaries, contrary to the suggestion that power-law-dominated spectra of ULXs originate in the very high state. A simple interpretation of this is that we are observing accretion on to intermediate-mass black holes, though we might also be observing a spectral state unique to very high mass accretion rates in stellar-mass black hole systems. Short-term flux variability is only detected in one of two epochs for two of the ULXs, with the lack of this characteristic arguing that the X-ray emission of this sample of ULXs is not dominated by relativistically beamed jets. The observational characteristics of this small sample suggest that ULXs are a distinctly heterogeneous source class.

Key words: black hole physics – X-rays: binaries – X-rays: galaxies.

1 INTRODUCTION

Ultraluminous X-ray sources (ULXs) can be broadly defined as the most luminous point-like extranuclear X-ray sources located within nearby galaxies, displaying X-ray luminosities in excess of 10^{39} erg s^{-1}. These sources were first observed in *Einstein* observations of nearby galaxies (e.g. Fabbiano & Trinchieri 1987) and more than one hundred were subsequently catalogued in *ROSAT* High Resolution Imager (HRI) observations (Roberts & Warwick 2000; Colbert & Ptak 2002). Whilst a fraction of this observed ULX population is associated with recent supernovae (e.g. SN 1986J, Bregman & Pildis 1992; SN 1979C, Immler, Pietsch & Aschenbach 1998), *ASCA* studies have shown that many ULXs appear to display the characteristics of accreting black holes (e.g. Makishima et al. 2000; Mizuno, Kubota & Makishima 2001). Crucially, high spatial resolution *Chandra* observations (e.g. Kaaret et al. 2001; Strickland et al. 2001) have failed to resolve most ULX targets. When combined with the observed significant flux variability, this suggests the presence of a single, luminous source of X-rays rather than a grouping of less luminous sources.

However, debate over the nature of the bulk of the ULX population is ongoing because if these are accretion-powered sources then their X-ray luminosities match, and in many cases greatly exceed, the Eddington limit for a typical stellar-mass ($\sim$10 M$_\odot$) black hole. Suggestions for their physical composition currently focus upon four possibilities. The first is that many ULXs are accreting examples of a new class of 10^2–10^5 M$_\odot$ intermediate-mass black holes (IMBHs: e.g. Colbert & Mushotzky 1999). The formation of such objects remains a matter of some debate: some IMBHs may be the remnants of primordial Population III stars (e.g. Madau & Rees 2001), whilst others may be formed in dense globular clusters prior to being deposited in a galaxy disc (Miller & Hamilton 2002). An alternative scenario is that IMBHs are formed by the runaway merger of stellar objects at the centre of young, dense stellar clusters (Ebisuzaki et al. 2001; Portegies Zwart & McMillan 2002). The existence of IMBHs may be supported by the recent inference of 3×10^3 and 2×10^4 M$_\odot$ massive dark objects in the cores of the globular

★E-mail: tro@star.le.ac.uk

Table 1. Details of the 10 *Chandra* observations.

Target	Observation aimpoint RA	Dec.	*Chandra* sequence number	Observation date (yyyy-mm-dd)	ACIS-S3 sub-array	Exposure (ks)
IC 342 X-1	$03^{h}45^{m}55\overset{s}{.}2$	$+68^{\circ}04'55''$	600253	2002-04-29	$\frac{1}{8}$	9.9
			600254	2002-08-26		9.9
NGC 3628 X-2	$11^{h}20^{m}37\overset{s}{.}5$	$+13^{\circ}34'28''$	600255	2002-04-06	full	22.3
			600256	2002-07-04		22.5
NGC 4136 X-1	$12^{h}09^{m}22\overset{s}{.}6$	$+29^{\circ}55'49''$	600257	2002-03-07	full	18.8
			600258	2002-06-08		19.7
NGC 4559 X-1	$12^{h}35^{m}52\overset{s}{.}0$	$+27^{\circ}56'01''$	600160	2001-01-14	$\frac{1}{4}$	9.7
			600161	2001-06-04		11.1
NGC 5204 X-1	$13^{h}29^{m}39\overset{s}{.}2$	$+58^{\circ}25'01''$	600162	2001-01-09	$\frac{1}{8}$	10.1
			600163	2001-05-02		9.5

clusters M15 and G1, respectively (van der Marel et al. 2002; Gerssen et al. 2002; Gebhardt, Rich & Ho 2002), though the presence of such an object in M15 is far from proven (Baumgardt et al. 2003). Further evidence has recently emerged with the discovery of the X-ray spectral signature of cool accretion discs, consistent with the presence of IMBHs, in several ULXs (e.g. Miller et al. 2003a; Roberts & Colbert 2003).

The remaining models focus upon interpreting ULXs as extreme examples of ordinary stellar-mass (i.e. $\sim$10 $M_{\odot}$) black hole X-ray binaries. The second physical model is that many ULXs are ordinary X-ray binaries in an unusually high accretion mode, in which their accretion disc becomes radiation pressure dominated, producing photon bubble instabilities that allow the disc to radiate at a truly super-Eddington X-ray flux (Begelman 2002). The third model is that many ULXs may only appear to exceed the Eddington limit, but they could in fact be X-ray binaries emitting anisotropically (King et al. 2001), with only a mild beaming factor $b \sim 0.1$ (where $b = \Omega/4\pi$ and Ω is the solid angle of the X-ray emission) required in most cases to reduce the energy requirements below the Eddington limit for a conventional stellar-mass black hole. The fourth model is a variation on the third scenario, suggested by Reynolds et al. (1997) and more recently Körding, Falcke & Markoff (2002) and Georganopoulos, Aharonian & Kirk (2002), in which ULXs are microquasars in nearby galaxies that we are observing directly down the beam of their relativistic jet (microblazars, cf. Mirabel & Rodriguez 1999). Observational support for this last scenario comes from the detection of radio emission, potentially the signature of a relativistically beamed jet, emanating from a ULX in NGC 5408 (Kaaret et al. 2003).

Current observations do not completely rule out any of the above scenarios. However, they do suggest that there may be at least two separate underlying populations of ULXs because a large number are seen coincident with active star formation regions (e.g. Zezas & Fabbiano 2002; Roberts et al. 2002), and hence are presumably associated with nascent stellar populations, whereas some ULXs are found in elliptical galaxies (e.g. Irwin, Athey & Bregman 2003) and so must be associated with an older stellar population. King (2002) suggests that the populations associated with star formation are high-mass X-ray binaries (HMXBs) undergoing an episode of thermal-time-scale mass transfer (see also King et al. 2001), whilst the older population may be long-lasting transient outbursts in low-mass X-ray binaries. Local examples of each suggested class are SS 433 and GRS 1915+105, respectively. This heterogeneity is supported by the first reported optical stellar counterparts to ULXs. Roberts et al. (2001) report the detection of a blue continuum source coincident with NGC 5204 X-1, which *HST* resolved into three separate sources with colours that are consistent with young, compact stellar clusters in NGC 5204 (Goad et al. 2002). *HST* observations also show a ULX in M81 (NGC 3031 X-11) to have a possible O-star counterpart (Liu, Bregman & Seitzer 2002a). In contrast, ULXs have been found with potential globular cluster counterparts in both NGC 4565 (Wu et al. 2002) and 1399 (Angelini, Loewenstein & Mushotzky 2001), suggesting that these ULXs are associated with the older stellar population, or perhaps massive central black holes, of these globular clusters.

In this paper, we present the results of dual-epoch *Chandra* observations of five different ULXs located in nearby ($d < 10$ Mpc) galaxies, awarded *Chandra* time in AO-2 and AO-3. These ULXs are listed in Table 1. They were selected from the catalogues of *ROSAT* HRI point-like X-ray source detections in nearby galaxies presented by Roberts & Warwick (2000, hereafter RW2000) and Lira, Lawrence & Johnson (2000) on the basis of their high X-ray luminosities ($L_{\rm X} > 10^{39}$ erg s^{-1} in the *ROSAT* HRI) and the lack of previous *Chandra* observations. A discussion of the observational history of these ULXs is presented in Appendix A. Further discussion of the environment of each of these ULXs, as determined from William Herschel Telescope/INTEGRAL IFU observations, will be detailed in a future paper (Roberts et al., in preparation).

The layout of this paper is as follows. In the next section we briefly outline the details of the *Chandra* observations and the data reduction. This is followed by a discussion of the detection of these (and three other) ULXs and their locations within their host galaxies. In Section 4 we detail the spatial, temporal and spectral properties of each source, before discussing the implications of these results for possible physical models of ULXs in Section 5. Our findings and conclusions are summarized in Section 6.

2 *CHANDRA* OBSERVATIONS AND DATA REDUCTION

The details of the 10 *Chandra* observations of ULXs that form the basis of this paper are listed in Table 1. The observations were pointed at the *ROSAT* HRI positions of the ULXs, after a correction to the astrometry calculated from X-ray/optical matches in the HRI field of view. All coordinates listed in Table 1, and throughout this paper, are epoch J2000. We tabulate some basic parameters for the host galaxies in Table 2. The observations were performed between 2001 January 9 and 2002 August 26, and range in exposure time from 9.7 to 22.5 ks. Each target was observed on two occasions, separated by 3–5 months. In order to mitigate the anticipated effects of detector pile-up in the ACIS-S S3 chip, several of the

Table 2. The host galaxies.

Galaxy	Hubble type[a]	d^b (Mpc)	i^b (°)	$N_{\rm H}^c$ ($\times 10^{20}$ cm^{-2})
IC 342	SAB(rs)cd	3.9	20	30.3
NGC 3628	SAb pec sp	7.7	87	2.0
NGC 4136	SAB(r)c	9.7	0[d]	1.6
NGC 4559	SAB(rs)cd	9.7	69	1.5
NGC 5204	SA(s)m	4.8	53	1.5

[a]Data from the NASA/IPAC Extragalactic Database (NED).
[b]Distance (d) and inclination (i) data from Tully (1988).
[c]Foreground absorption, interpolated at the position of each galaxy from the H I maps of Stark et al. (1992).
[d]There is no recorded inclination, so a face-on aspect is adopted after inspection of Digitized Sky Survey images.

observations were performed in a sub-array mode: these are listed in Table 1. The choice of sub-array was governed by the anticipated count rates, modelled from the previous *ROSAT* HRI observations of these objects (RW2000; Lira et al. 2000), with the aim of limiting the pile-up fraction to 10 per cent or less in each observation. On this basis, sub-arrays were deemed necessary for three of the five targets in the programme.

Data reduction was performed using the CIAO software suite, versions 2.1 and 2.2. The reduction started in each case with the level two event file, from which events with energies outside the 0.3–10 keV range were rejected. All data sets were searched for periods of high background flaring but none was observed, allowing the full science exposure to be utilized in each case. Further steps in the analysis of the data are outlined in the following sections.

3 ULX DETECTIONS AND LOCATIONS

A 0.3–10 keV image of the central 8.1 × 8.1 arcmin^2 region of each field was constructed from the corresponding cleaned event file. This image was searched for point sources using WAVDETECT, a wavelet-based source detection algorithm available in the CIAO package, and the X-ray source detections coincident with the optical extent of each galaxy (or that part of it within the ACIS-S3 field of view) were catalogued. The target ULXs were detected in every observation and their *Chandra* nomenclature,[1] including their refined position, and observed count rates are listed in Table 3. Count rates were converted to approximate fluxes based on a simple power-law continuum model with a standard photon index (Γ) of 2, subject to a foreground absorption column appropriate for each galaxy (see Table 2). In addition to the targets, three other sources with luminosities potentially in the ULX regime were found: one is a previously catalogued source (NGC 4559 X-4 in RW2000), but the other two are new ULX identifications. The details of these new ULXs are also given in Table 3.

One excellent capability of the *Chandra* observatory is that it provides an absolute astrometry solution to an accuracy of 1 arcsec or better. This positional accuracy facilitates detailed follow-up of the *Chandra* X-ray source detections through the characterization of their multi-wavelength counterparts. This avenue has already borne fruit in the study of ULXs, as discussed in the introduction. Here, however, we limit ourselves to a brief discussion of the environment of the *Chandra* ULX detections on the basis of Palomar Digitized Sky Survey (DSS) data.

The positions of the ULXs relative to their host galaxies are illustrated in Fig. 1, where we overlay the *Chandra* X-ray emission contours on to DSS-2 (blue) images of the equivalent field of view. In each case the target ULX is at the centre of the field of view. The position of each ULX with respect to the nucleus of the parent galaxy is quantified in Table 3. The observed offset from the position of the galaxy nucleus, taken in each case from Falco et al. (1999), is simply the projected distance measured in arcseconds: we correct this to a deprojected radius, assuming that each source is in the plane of its host galaxy, using the host's inclination as given in Table 2 and a position angle taken from the RC3 catalogue (de Vaucouleurs et al. 1991). This deprojected radius is also shown as $f(R_{25})$, the fraction of the distance between the nucleus and the edge of the galaxy, defined by the semimajor axis of the 25 mag arcsec^{-2} isophotal ellipse, at which the ULX is found. Finally, we also give a qualitative description of the region of the galaxy in which the ULX is found.

If the ULXs in these galaxies are associated with young stellar populations, we might expect to find them co-located with the regions of the galaxy most prone to hosting star formation, such as the spiral arms, whereas if they are associated with the older stars then their distribution is more likely to be centrally peaked, or spread evenly throughout the disc. Table 2 shows that the majority of the ULXs (five out of eight) are located more than halfway out from the nucleus towards the edge of the galaxy. Four of these five appear coincident with spiral arms; the fifth (CXOU J112037.3+133429) is located in an edge-on system where we cannot distinguish whether it is in an arm or inter-arm region.

The identification of four of the ULXs with spiral arms is relatively robust, as in both IC 342 and NGC 4136 the galaxies are face-on and so line-of-sight confusion through the galaxy is minimized. This is also true for CXOU J123551.7+275604 in NGC 4559, as this is located in a faint outer spiral arm clearly separated in projection from the main body of the galaxy. The co-location of the ULXs with spiral arms argues that they could be associated with a young stellar population. If they are ordinary X-ray binaries, with typical kicks imparted from the formation of the compact primary in a supernova explosion of $\sim$100 km s^{-1} (cf. recent results for GRO 1655 − 40: Mirabel et al. 2002), then in 10^7 yr this would move the position of the ULX relative to its birth place by a maximum of 1 kpc, consistent with an observed position in or near a spiral arm if born there. However, if the ULXs are associated with an older population then in their $>10^8$ yr lifetime, they could be displaced by 10 kpc or more, clearly leaving no requirement for an association with the spiral arms. The arguments in favour of these ULXs being related to young stellar populations are supported by follow-up observations of the immediate environments of three of these outer ULXs, with H II regions detected close to (within 200 pc of) CXOU J123551.7+275604 and coincident with CXOU J120922.6+295551 (Roberts et al., in preparation), and the detection of a possible supernova remnant encircling the position of CXOU J034555.7+680455 (Roberts et al. 2003). However, the kick argument above requires that the ULXs either are very young, or possess a small kick velocity and/or a velocity almost entirely projected along our line of sight for these to be true physical associations rather than line-of-sight coincidences with the star formation regions that we might expect to observe within the spiral arms of a galaxy.

Line-of-sight confusion is a much bigger issue for the three ULXs that are located closer to the centre of their respective host galaxies.

[1] We refer to the ULXs by their *Chandra* names throughout this paper. The cross-identification with previous names is shown where necessary.

Table 3. The ULX detections.

CXOU J	Previous designation	Count rate (count ks^{-1}) Epoch 1	Epoch 2	Offset from galaxy nucleus Observed (arcsec)	Deprojected (kpc)	$f(R_{25})$	Location
Targetted ULX							
034555.7+680455	IC 342 X-1	212 ± 5	226 ± 5	302	6.1	0.68	Spiral arm
112037.3+133429	NGC 3628 X-2	13 ± 1	13 ± 1	292	10.8	0.66	Outer disc
120922.6+295551	NGC 4136 X-1	3 ± 1	4 ± 1	65	3.0	0.54	Spiral arm
123551.7+275604	NGC 4559 X-1	153 ± 4	192 ± 4	123	15.2	0.96	Faint outer spiral arm
132938.6+582506	NGC 5204 X-1	411 ± 6	159 ± 4	17	0.7	0.21	Inner disc
Field ULX							
120922.2+295600	–	26 ± 1	18 ± 1	62	2.9	0.52	Spiral arm
123557.8+275807	–	11 ± 1	21 ± 1	31	2.3	0.15	Inner disc
123558.6+275742	NGC 4559 X-4	62 ± 3	119 ± 3	12	1.7	0.11	Inner disc/bulge

Despite this, detailed follow-up of CXOU J132938.6+582506 reveals it to be associated with young stars (Goad et al. 2002). The remaining two sources are located close to the centre of NGC 4559. However, the nucleus of this galaxy is known to host active star formation (Ho, Filippenko & Sargent 1997), implying that it is possible (though by no means certain) that these ULXs may also be related to the presence of young stars. It is entirely plausible, therefore, that all the ULXs in this small sample may be associated with young stellar populations. This is consistent with previous studies finding comparatively large populations of ULX in the most active star-forming galaxies (e.g. Fabbiano, Zezas & Murray 2001; Lira et al. 2002; Zezas, Ward & Murray 2003), indicating a relationship between many ULXs and active star formation, though interestingly in this case we co-locate them with the star-forming regions of otherwise relatively normal galaxies.

To put this in context, it is worth noting that the host galaxies in our sample are all type Sb or later, indicating that they are disc-dominated, and so do not possess large bulges dominated by old stars. We can investigate the ULX–young stellar population link further by reference to the ULX survey of Colbert & Ptak (2002). They detect more than 30 candidate ULXs coincident with, or in the haloes of, elliptical galaxies, which must be dominated by an old stellar population. Averaging over the 14 elliptical galaxies in which ULXs are located with respect to the blue luminosity of each galaxy, L_B, gives 0.8 ULX per $10^{10} L_B$. This is very much an upper limit on the number of ULX from an old stellar population, as Colbert & Ptak (2002) search out to a radius of $2R_{25}$, potentially allowing a much greater contamination from background objects than simply focusing within the standard definition of the galaxy size, the 25 mag arcsec^{-2} isophotal ellipse. Also, because many of their candidate ULXs are possible halo objects, these may, therefore, constitute a physically separate population to that associated with the old stellar population. Nevertheless, by comparing their average ULX to L_B ratio with the blue luminosities of our target galaxies (and correcting for the coverage of each galaxy in the *Chandra* observations), we can establish a conservative upper limit on the number of our ULXs associated with the older stellar populations. This turns out to be an upper limit of two out of the eight ULXs we observe. We therefore confirm that our sample is very likely to be dominated by ULXs associated with a young stellar population.

4 X-RAY CHARACTERISTICS

In this section we investigate the detailed X-ray properties of the sources. Unless specifically stated, we perform the analyses on all five target plus all three field ULXs. Discussion of these characteristics in terms of physical models is deferred until later sections.

4.1 Spatial extent

A primary goal of this programme was to use the unique 0.5 arcsec spatial resolution of *Chandra* to investigate whether these ULXs are resolved into complexes of many X-ray emitting sources, or whether they remain a single, point-like object at the highest available X-ray resolution. Hence, the target ULXs were placed at the on-axis aim point of the ACIS-S3 chip in each observation to provide the best possible spatial data.

To investigate the question of spatial extension, the two observations of each field were combined to enhance the signal-to-noise ratio of the images. The excellent spatial precision of the data (1 pixel $\equiv 0.492$ arcsec) was maintained by aligning the peak in intensity of each target source. This method was verified by examining the peaks in fainter sources within the field, which also aligned accurately. We then derived the radial profile of each ULX and fitted its core with a Gaussian function, following the procedure described in section 4.2.1 of Roberts et al. (2002).[2] The resulting fits gave FWHM of between 1.8 and 2.2 pixel for all on-axis sources, and ∼2.4 pixel for the 2-arcmin off-axis ULXs in NGC 4559, all consistent with the nominal *Chandra* point-spread function at those positions. No evidence was found for a faint, extended component surrounding the position of any of the ULXs. This demonstrates that the ULXs are point-like at the 0.5-arcsec spatial resolution of *Chandra*, corresponding to maximum physical sizes for the X-ray emitting regions of ∼9–23 pc in the host galaxies. The spatial data are also, of course, consistent with all the objects being single, point-like X-ray sources.

4.2 Spectral properties

Spectra were extracted in an 8 arcsec diameter aperture centred on the position of each ULX using the PSEXTRACT script, which also retrieves the appropriate response matrices and ancillary response files for each observation. A source-free local background region of equivalent size was used in each case, though its impact was of little significance because it typically contained only 0.1–1 per cent of the counts accumulated from the source. The ancillary response files were corrected for the gradual in-orbit degradation in the quantum efficiency of the ACIS detectors using the CORRARF tool.[3] The spectra were grouped to a minimum of 20 counts per bin, and then analysed in XSPEC v.11.2, excluding data below 0.5 keV as a result of

[2] Some adjustments to the size and position of the background annuli were required to eliminate nearby X-ray sources in several fields. An example is the NGC 4136 field, in which the two ULXs are separated by only ∼22 pixel.
[3] See http://asc.harvard.edu/cal/Acis/Cal_prods/qeDeg

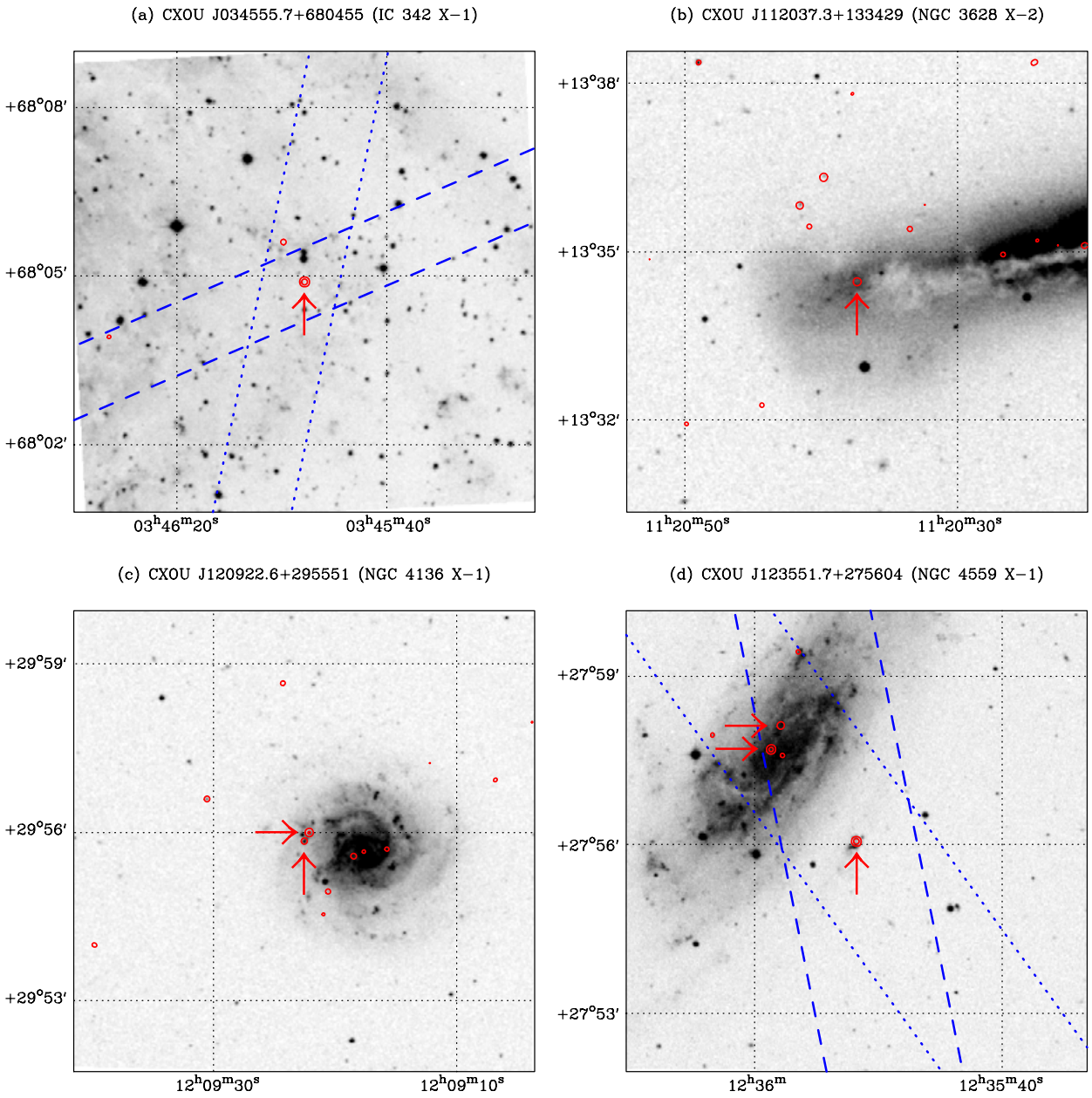

Figure 1. The locations of the five target ULXs. Each figure shows an 8.1 × 8.1 arcsec^2 DSS-2 blue image centred on the position of the ULX, rotated slightly to match the *Chandra* projection. Coordinates are shown in J2000. The *Chandra* X-ray emission contours are overlaid in red to highlight the positions of the X-ray sources in each field of view. The *Chandra* data have been smoothed by a HWHM 3-pixel Gaussian mask to aid visibility and the contours are plotted at 0.3 and 10 count pixel^{-1}. The target and field ULXs are highlighted by the vertical and horizontal arrows, respectively. The spatial coverage of the *Chandra* sub-arrays used for observations of the IC 342 X-1 and NGC 4559 X-1 fields are highlighted in blue for each respective field, with the first- and second-epoch coverage shown by the dashed and dotted lines, respectively.

the uncertainty in the calibration at these energies. In the following analysis, all quoted errors are the 90 per cent confidence errors for one interesting parameter.

A major consideration in the design of these observations was to limit the distorting effect of detector pile-up on the observed X-ray spectrum of each ULX. As stated in Section 2, the *ROSAT* HRI count rates of each ULX were used to determine the optimum sub-array size to lower the anticipated pile-up fraction below 10 per cent. However, this did not guarantee that each source would have an acceptable level of pile-up, as a result of the long-term variable nature of the ULXs themselves (see below). We can derive a lower limit on the observed pile-up fraction of each observation by reference to fig. 6.24 of the *Chandra* Proposer's Observatory Guide (v.4),[4] which shows pile-up fraction as a function of counts per readout frame (we calculate a lower limit because our input is the observed counts per frame, which already includes piled-up events). This is very much a first-order approximation, because it does not include, for example, the effect of variations in the source spectra on the degree of pile-up. Only one observation, the 2001 January

[4] See http://asc.harvard.edu/proposer/POG/index.html

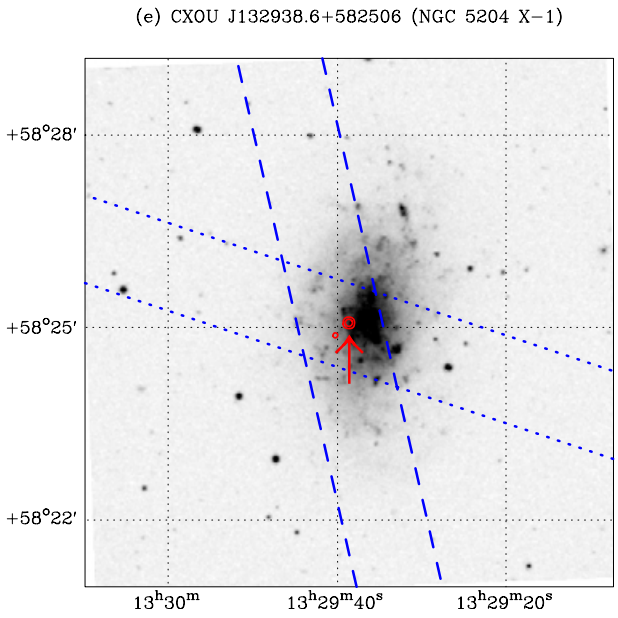

Figure 1 – *continued*

observation of CXOU J132938.6+582506, turns out to have a lower limit in excess of 10 per cent and this is only marginal at 11 per cent. All other observations have limits of 8 per cent pile-up or less, implying that the policy of using sub-arrays was successful.

We investigated the presence of residual pile-up effects using the XSPEC v.11.2 parametrization of the CCD event pile-up model of Davis (2001). A simple absorbed power-law continuum model, both with and without the pile-up model, was fitted to the observed spectrum of the brightest ULXs (namely CXOU J132938.6+582506, CXOU J123551.7+275604 and CXOU J034555.7+680455 in both epochs, and CXOU J123558.6+275742 in its second observational epoch). In the pile-up model we allowed α, the grade-morphing parameter, to vary freely and set the frame time to 0.7 and 1.1 s for the 1/8 and 1/4 sub-arrays, respectively, with the other parameters fixed as default. In six of the seven cases, the changes to the spectral fit when the pile-up algorithm was applied were minimal ($\Delta\chi^2 < 3$ for one extra degree of freedom). Though in most cases the power-law photon indices became slightly softer, as expected because CCD pile-up acts to harden the observed source spectra, this change was offset by much worse constraints on the parameters. Hence, the absorption columns and power-law photon indices were consistent both with and without the inclusion of the pile-up model, within the derived errors, in all six cases. None of these six fits was able to place strong constraints on α. We therefore consider pile-up effects to be negligible in the X-ray spectra of all except one of the ULXs.

The only case in which the pile-up model gave a much improved χ^2 was the 2001 January observation of CXOU J132938.6+582506, with $\Delta\chi^2 = 16.3$ for one extra degree of freedom, and a statistically significant softening of the spectral slope. We discuss this case further below.

The ULX observations in which fewer than 250 source counts were accumulated were not considered for spectral analysis, which ruled out both observations of CXOU J120922.6+295551 and CXOU J123557.8+275807. The remaining spectra were initially fitted with simple absorbed single-component spectral models, namely a power-law continuum, a thermal bremsstrahlung model, the multicolour-disc blackbody model (hereafter MCDBB) used to describe an accretion disc around a black hole in its high (soft) state (Mitsuda et al. 1984), a MEKAL optically thin thermal plasma model, and a conventional blackbody spectrum. The best-fitting parameters to the power-law continuum and MCDBB models are listed in Table 4 and individual cases are discussed below. The thermal bremsstrahlung model provided an adequate fit in most cases,

Table 4. Best fits of two simple models to the two-epoch ULX X-ray spectra.

ULX (CXOU J)	Epoch	WA*PO[a]			WA*DISKBB[a]			L_X[b]
		N_H[c]	Γ[d]	χ^2/d.o.f.	N_H[c]	kT_{in}[e]	χ^2/d.o.f.	
034555.7+680455	2002-04-29	0.52 ± 0.07	$1.63^{+0.13}_{-0.12}$	**78.8/81**	$0.30^{+0.05}_{-0.04}$	$1.81^{+0.22}_{-0.18}$	97.4/81	4.4(5.9)
	2002-08-26	0.61 ± 0.08	$1.70^{+0.12}_{-0.13}$	**92.0/87**	0.36 ± 0.05	$1.76^{+0.19}_{-0.16}$	105.7/87	4.4(6.4)
112037.3+133429	2002-04-06	0.022[f]	1.57 ± 0.24	**8.4/10**	0.022[f]	$0.95^{+0.3}_{-0.2}$	12.3/10	0.7(0.8)
	2002-07-04	$0.16^{+0.09}_{-0.13}$	$2.20^{+0.34}_{-0.19}$	**4.4/10**	0.022[f]	$0.86^{+0.18}_{-0.14}$	6.4/11	0.6(0.7)
120922.2+295600	2002-03-07	$0.13^{+0.08}_{-0.07}$	$1.68^{+0.27}_{-0.22}$	**30.1/19**	0.016[f]	$1.46^{+0.27}_{-0.25}$	37.7/20	2.3(2.6)
	2002-06-08	<0.21	$1.55^{+0.30}_{-0.33}$	**13.9/13**	0.016[f]	$1.43^{+0.44}_{-0.24}$	18.4/14	1.7(1.9)
123551.7+275604	2001-01-14	0.015[f]	1.91 ± 0.09	**69.9/52**	0.015[f]	[~ 0.84][g]	169/52	9.8(10.0)
	2001-06-04	0.04 ± 0.03	$2.16^{+0.15}_{-0.14}$	**100/72**	0.015[f]	[~ 0.66][g]	222/73	11.6(12.5)
123558.6+275742	2001-01-14	$0.17^{+0.08}_{-0.07}$	$1.98^{+0.23}_{-0.24}$	26.3/22	0.015[f]	$1.14^{+0.15}_{-0.13}$	**24.6/23**	4.2(4.3)
	2001-06-04	0.16 ± 0.06	$1.82^{+0.17}_{-0.15}$	63.6/51	0.015[f]	$1.30^{+0.12}_{-0.10}$	**49.2/52**	8.9(9.1)
132938.6+582506	2001-01-09	0.10 ± 0.02	$2.38^{+0.10}_{-0.11}$	**141/109**	0.014[f]	[~ 0.7][g]	260/110	5.7(6.9)
	2001-05-02	$0.10^{+0.05}_{-0.04}$	$2.96^{+0.25}_{-0.21}$	**41.1/46**	0.014[f]	$0.44^{+0.04}_{-0.03}$	86.5/47	1.8(2.4)

[a]Spectral model components are shown as per the XSPEC syntax with: a cold absorption model (WA), a power-law continuum (PO) and the MCDBB model (DISKBB).
[b]Observed luminosity in the 0.5–8 keV band in units of 10^{39} erg s^{-1}. Figures in parentheses give the intrinsic (unabsorbed) luminosity. We calculate these values using the best-fitting model highlighted by showing its χ^2/d.o.f. in bold.
[c]Absorption column, in units of 10^{22} atom cm^{-2}.
[d]Power-law photon index.
[e]Inner accretion disc temperature in keV.
[f]Value fixed at the foreground Galactic absorption column (see Table 2).
[g]Parameter value not constrained by model fit.

Table 5. Two-component fits to the ULX X-ray spectra.

ULX (CXOU J)	Epoch	Model[a]	α	$N_{\rm H}$	$kT/kT_{\rm in}$	Γ	χ^2/d.o.f.	$\Delta\chi^{2b}$
120922.2+295600	2002-03-07	WA*(DISKBB+PO)	–	$0.81^{+0.37}_{-0.34}$	$0.12^{+0.05}_{-0.04}$	$1.77^{+0.36}_{-0.34}$	16.7/17	13.4
123551.7+275604	2001-01-14	WA*(DISKBB+PO)	–	<0.25	$0.20^{+0.15}_{-0.07}$	$1.71^{+0.23}_{-0.16}$	65.0/49	4.9
	2001-06-04	WA*(DISKBB+PO)	–	$0.19^{+0.08}_{-0.14}$	$0.15^{+0.10}_{-0.03}$	$2.10^{+0.18}_{-0.26}$	92.4/70	7.6
		WA*(MEKAL+PO)	–	$0.41^{+0.13}_{-0.19}$	$0.18^{+0.05}_{-0.02}$	$2.34^{+0.10}_{-0.14}$	76.7/70	23.3
132938.6+582506	2001-01-09	PILEUP*WA*PO	$0.57^{+0.32}_{-0.18}$	0.14 ± 0.03	–	$2.79^{+0.16}_{-0.14}$	124/108	16.3

[a]The model components and parameters are as in Table 4, except for the MEKAL component, which is a thermal plasma model with its metallicity fixed at solar abundance, and PILEUP which is as described in the text.
[b]Improvement in the χ^2 statistic over the single-component model best fit, for two extra degrees of freedom (one extra in the pile-up model).

though never as statistically acceptable as a power-law continuum (or MCDBB in the case of CXOU J123558.6+275742). We omit it from the table in favour of the two models that have more generally been used to describe ULX spectra in past analyses. The spectra were generally too hard to provide meaningful fits to the MEKAL model, whose parameters tended towards those of the thermal bremsstrahlung fit. Similarly, simple blackbody models did not provide a good fit to any of the spectra.

As shown in Table 4, most data sets are adequately described by a single (absorbed) spectral model component, with a reduced χ^2 value at, or below, unity. However, in several instances the reduced χ^2 is still considerably above 1. We have attempted to fit these data sets with more complex two-component models (see Table 5). All three data sets for which the spectral fit was improved by the addition of a second spectral component (excluding the pile-up correction to CXOU J132938.6+582506) required the presence of a very soft spectral component. These are discussed on a case-by-case basis in the following subsections, where we discuss the spectral fits to each individual ULX. We demonstrate the spectral quality of each observation of each source in Figs 2 and 3. These show the data and the best-fitting single-component model in the upper window of each panel, and the residuals when the data is divided by the best-fitting model in the lower panel.

4.2.1 CXOU J034555.7+680455 (IC 342 X-1)

This ULX showed a fairly constant X-ray spectrum between the two observations, with an absorbed power-law continuum providing a good fit to the data from both epochs. In each case the absorption was roughly twice the foreground value (cf. Table 2), with the additional absorption of 2–3 $\times$ 10^{21} atom cm^{-2} in excess of the integrated column through IC 342 at the ULX position ($\sim$8 $\times$ 10^{20} atom cm^{-2}; Crosthwaite, Turner & Ho 2000). This implies a source of additional absorption intrinsic to, or in the environment of, CXOU J034555.7+680455. This may originate in the nebula surrounding this ULX described by Roberts et al. (2003). The *Chandra* spectra are consistent with the low/hard spectral state observed by *ASCA* in 2000 February 24–March 1, described by an absorbed power-law continuum with $N_{\rm H} = 0.64 \pm 0.07 \times 10^{22}$ atom cm^{-2} and $\Gamma = 1.73 \pm 0.06$ (Kubota et al. 2001). This state has also been interpreted as an anomalous/very high state (Kubota, Done & Makishima 2002), which we discuss further in Section 5.1. The luminosity also appears little changed at $\sim$5 $\times$ 10^{39} erg s^{-1} (versus 6 $\times$ 10^{39} erg s^{-1} in *ASCA*) when extrapolated to the 0.5–10 keV band. Hence, it appears that this ULX has been in a constant spectral state in three separate observations over 2.5 yr.

4.2.2 CXOU J112037.3+133429 (NGC 3628 X-2)

This ULX had faded to a luminosity of only $\sim$7 $\times$ 10^{38} erg s^{-1} in our *Chandra* observations, hence the spectra are of low quality, and the spectral models were not strongly constrained. A power-law continuum was again the preferred model in both epochs, though the MCDBB, also, gave a statistically acceptable fit in the second epoch. The source flux appeared to change little between the epochs, perhaps fading slightly in the three months between observations. However, despite the low quality, the intrinsic X-ray spectrum showed changes between the epochs, with the first observation showing an intrinsically hard ($\Gamma \sim 1.57$) but unobscured power-law continuum, whereas the second observation showed a softer intrinsic slope ($\Gamma \sim 2.2$) with a low-energy turnover as a result of absorption.

4.2.3 CXOU J120922.2+295600

This new ULX has a spectrum that is best fitted by a power-law continuum model in both epochs. However, the power-law fit is only statistically acceptable in the second epoch. In order to improve the fit to the first epoch data, we tried a variety of two-component spectral fits to the data. The best fits came from models with a highly absorbed, very soft component in addition to a hard power-law continuum. We show such a fit, with the very soft component modelled by a MCDBB, in Table 5. This fit is statistically acceptable for the data, and an improvement over the single power-law continuum model at 99.97 per cent ($>3\sigma$) confidence. Note, however, that the addition of a classical blackbody emission model (with kT = 0.1 keV) rather than a MCDBB model provides an equally acceptable fit to the data. The power-law continuum slope is consistent (within the large errors) in both epochs, though the inferred absorption column is much lower in the absence of a very soft component in the second observation.

4.2.4 CXOU J123551.7+275604 (NGC 4559 X-1)

This is the most luminous ULX in the sample, with its observed luminosity at, or above, 10^{40} erg s^{-1}. Its X-ray spectrum was observed to soften between the observations, with the X-ray emission in the second, more X-ray luminous epoch represented by a significantly softer power-law photon index than the first ($\sim$2.16 against $\sim$1.91). However, its X-ray spectrum is not well fitted by either simple model, with the MCDBB model rejected at high statistical significance. Two-component models incorporating a very soft MCDBB plus a power-law continuum offered improvements to the fit, as shown in Table 5, though only at the 69 and 94 per cent significance levels in the first and second epochs respectively. A classic

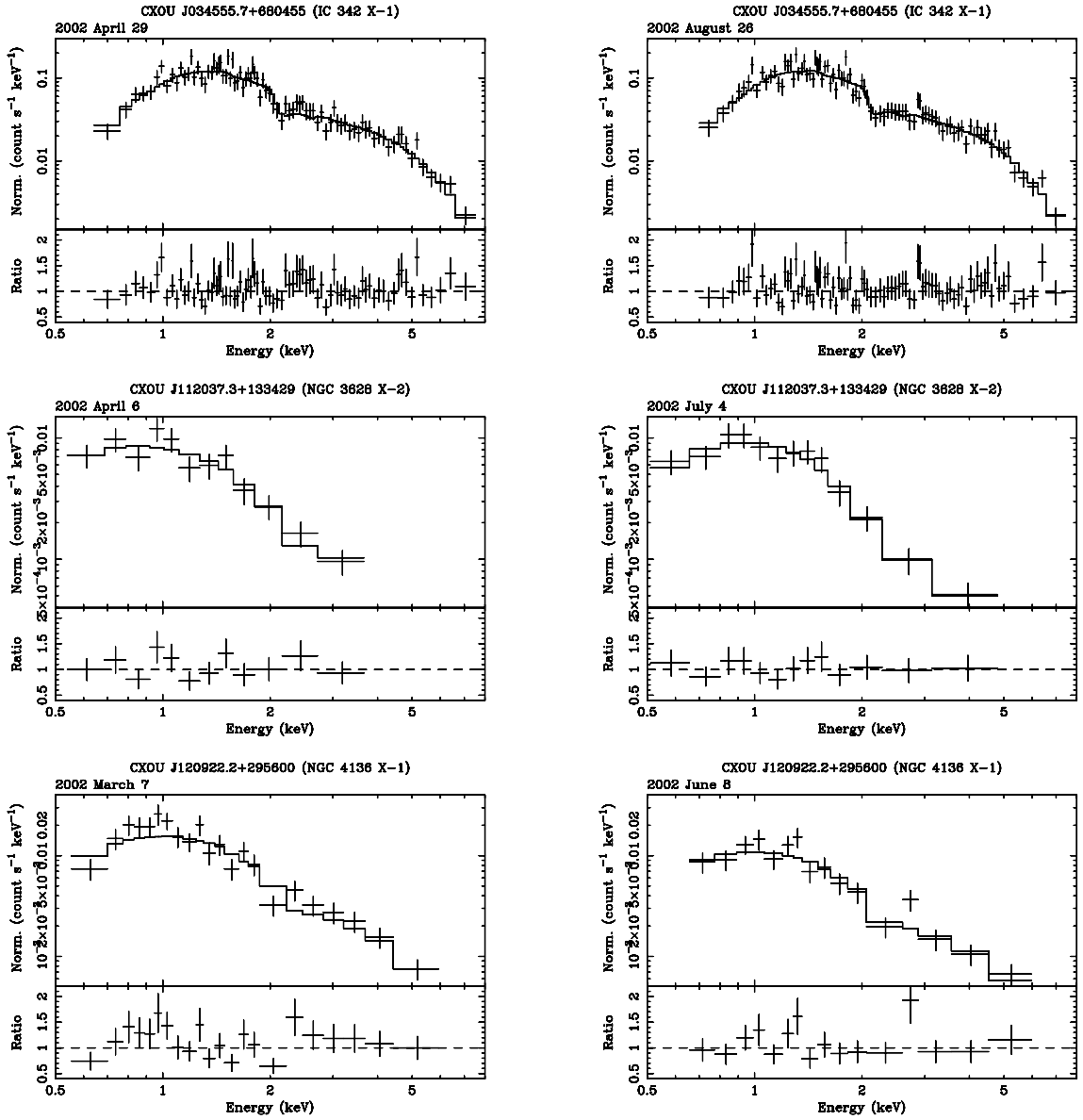

Figure 2. The *Chandra* ACIS-S3 spectra of the ULXs. We show the data and best-fitting single-component model in the top window of each panel and the ratio of the data to the model in the lower window. We plot the first- and second-epoch data for each ULX in the left and right columns, respectively, using the same normalization scaling for each pair of spectra to aid their direct comparison. All spectra are shown using the same energy scale and the ratio values are all displayed over the same range.

blackbody component offered a superior improvement in the second epoch, at the 96 per cent significance level according to the F-statistic.

Curiously, a substantial improvement in the fit to the second-epoch data was obtained when the MCDBB component was replaced with a MEKAL solar abundance thermal plasma with $kT \sim 0.18$ keV (Table 5). For two additional free parameters, the reduction in χ^2 of 23.3 implies a 99.99 per cent significance level (i.e. $>3.5\sigma$) in terms of the F-test. Fig. 4 shows the resulting best-fitting spectrum and the contribution of the MEKAL component. For comparison, a similar model (power-law plus $kT \sim 0.18$ keV MEKAL) was fitted to the first-epoch data and no significant improvement to the best fit was obtained, with the contribution of the putative thermal component limited to no more than 3 per cent of the 0.5–8 keV flux.

However, the MEKAL fit relies heavily on the fact that a blend of lines between 0.5 and 0.75 keV (predominantly O VII and O VIII), when combined with a factor ∼2 increase in the model $N_{\rm H}$, gives a good match to the additional soft emission apparent in the second-epoch spectrum. Is this thermal component real or simply an artefact of fitting a fairly complex model to data with limited spectral resolution and poor statistics (N.B. ∼600 counts out of ∼2000 in the full spectrum originate from the MEKAL component)? Clearly there is no direct evidence in the second-epoch spectrum for individual lines (though this is perhaps consistent with low temperature of the plasma and the >100 eV spectral resolution of the ACIS-S detector below 1 keV). On the other hand, when we allow the abundance of O, Ne and Fe (which produce the most significant line features in the $kT \sim 0.18$ keV plasma) to vary in the VMEKAL model, we obtain a best fit of 1.3 solar and a 90 per cent lower limit of 0.33 solar,

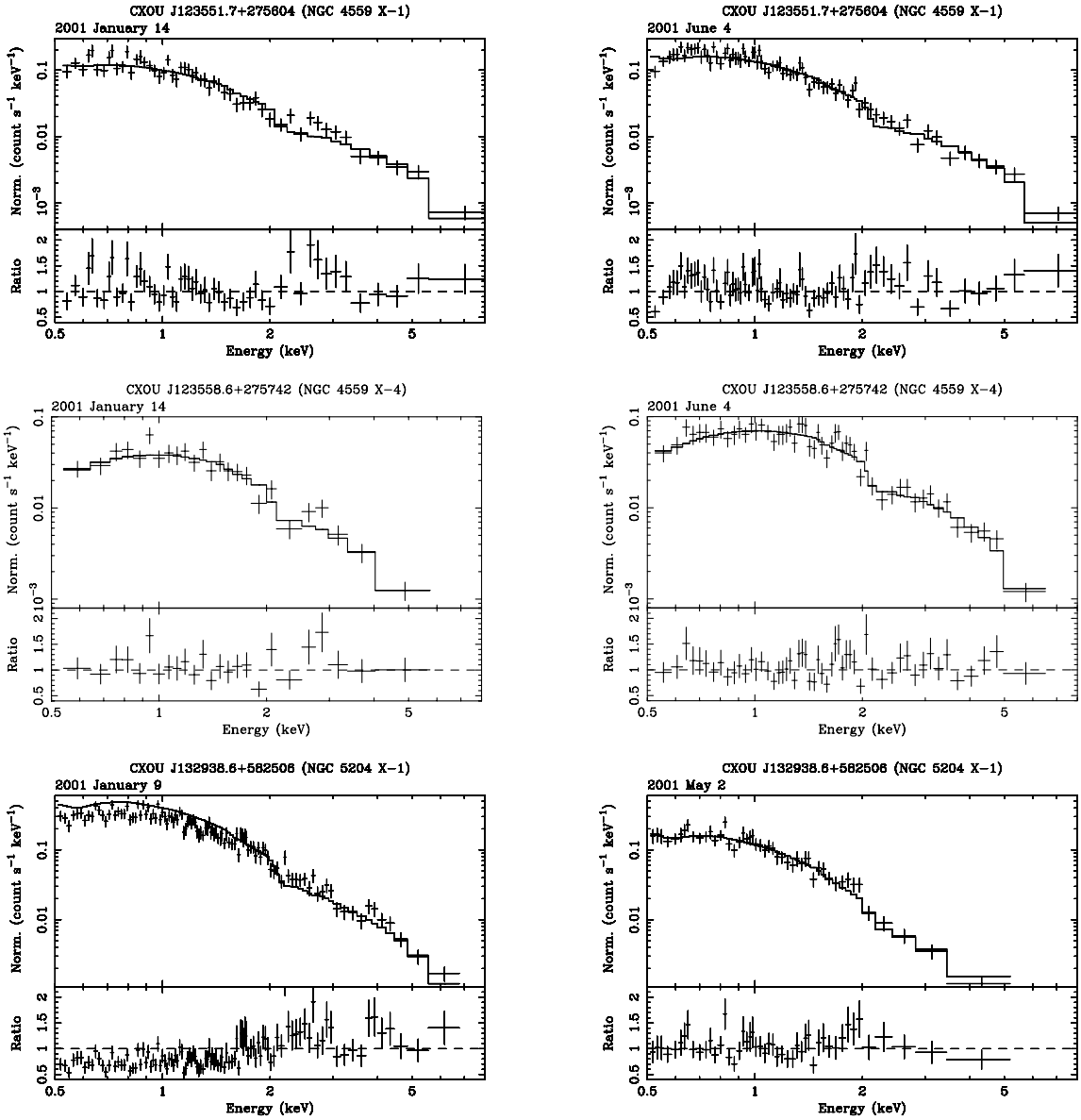

Figure 3. As for Fig. 2, except for the first-epoch spectrum of CXOU J132938.6+582506. Here, we plot the pile-up corrected spectral model over the actual data to demonstrate the degree of pile-up in the observed X-ray spectrum.

implying that there is a strong preference for a substantial contribution from emission lines. *However, this is on the basis of a spectral model that may not be correct*. We conclude that an interpretation of the additional soft flux present in the second epoch in terms of the emergence of a bright thermal component is potentially very interesting (see Section 5.3), albeit highly speculative.

Finally, we note that as this paper was undergoing the refereeing process these *Chandra* spectra were published by Cropper et al. (2004) as part of an *XMM–Newton* study of this source. They do not report the possible detection of a MEKAL component, though they did not explicitly look for it. Instead they fitted a particular model to the *Chandra* data, based on fits to the superior quality (and later epoch) *XMM–Newton* spectra, comprising a sub-solar-abundance absorber (TBVARABS, set at 0.31 times solar) applied to power-law plus blackbody emission components. We have applied the Cropper et al. model, plus variants incorporating soft MCDBB and MEKAL components, to the second-epoch spectrum and do get a marginal improvement in each case with respect to our original fits ($\Delta\chi^2 \sim$ 2–4); nevertheless the power-law plus MEKAL model still clearly provides the best result in terms of the minimum χ^2.

4.2.5 CXOU J123558.6+275742 (NGC 4559 X-4)

This object was the only ULX in the sample with an X-ray spectrum clearly best fitted with a MCDBB model. The inferred inner accretion disc temperatures were both greater than 1 keV, consistent with previous *ASCA* and some *Chandra* observations of ULX well fitted by this model (e.g. Colbert & Mushotzky 1999; Makishima et al. 2000; Roberts et al. 2002). The luminosity of the ULX more than doubles in the five months between observations, and this is associated with a slight hardening of the X-ray spectrum, with the best-fitting temperature of the inner accretion disc rising from ∼1.1 to ∼1.3 keV.

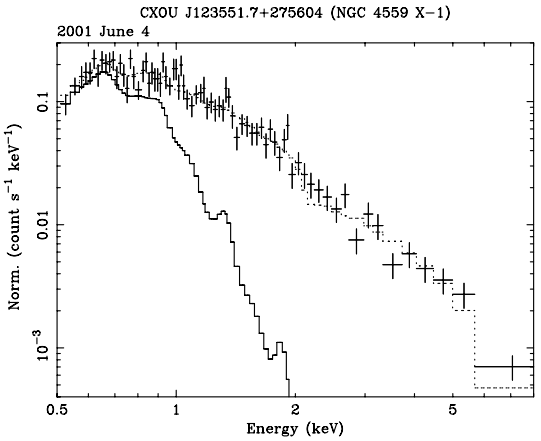

Figure 4. The second-epoch count-rate spectrum of CXOU J123551.7+275604. The best fit of the power law plus MEKAL model to the overall spectrum is shown as the dotted line with the contribution of the MEKAL component highlighted (solid line).

4.2.6 CXOU J132938.6+582506 (NGC 5204 X-1)

The X-ray spectrum of this ULX was far better fitted by a power-law continuum model than a MCDBB in both epochs, with it constituting a statistically acceptable fit in the second epoch. It was a poorer fit in the first epoch, though this observation was affected by a pile-up fraction in excess of 10 per cent of all events (see above). The XSPEC V.11.2 parametrization of the Davis (2001) pile-up correction model was used to correct for this effect, the results of which are shown in Table 5. This resulted in a much improved fit to a power-law continuum spectrum, with the inferred photon index softening considerably. Hence, whilst the two uncorrected spectra appear to have very a different hardness, after the correction for pile-up they are both revealed to be intrinsically very soft X-ray spectra. The photon indices of the power-law continuum fits are consistent within the errors after pile-up correction, albeit with a slightly harder value in the far more luminous first observation.

4.3 Temporal properties

4.3.1 Short-term variability

We derived short-term light curves for seven of the eight ULXs in both of their observation epochs, using the CIAO routine LIGHTCURVE. The exception was CXOU J120922.6+295551, which was too faint for this analysis with only 59 and 90 counts detected in total per epoch. Each light curve was binned to an average (over the observation) of 25 counts per bin, giving temporal resolutions ranging from ∼60, in the best case, to ∼2500 s. The resulting data were tested for gross variability using a χ^2 test against the hypothesis of a constant count rate. Five of the ULXs showed no strong evidence for short-term temporal variability in either epoch, with a reduced χ^2 statistic of 1.25 or less. However, two ULXs showed strong evidence for short-term variability in one of their two observation epochs. These light curves are plotted in Fig. 5. The appropriate χ^2/degrees of freedom statistics are 39.5/14 for the 2002 June observation of CXOU J120922.2+295600 (which had a 1407-s resolution) and 190/24 for CXOU J123558.6+275742 in its 2001 January observation (at 404-s resolution). The other observations of both sources were consistent with a constant flux, implying that the short-term variability states are themselves a transient phenomenon. These highly variable states

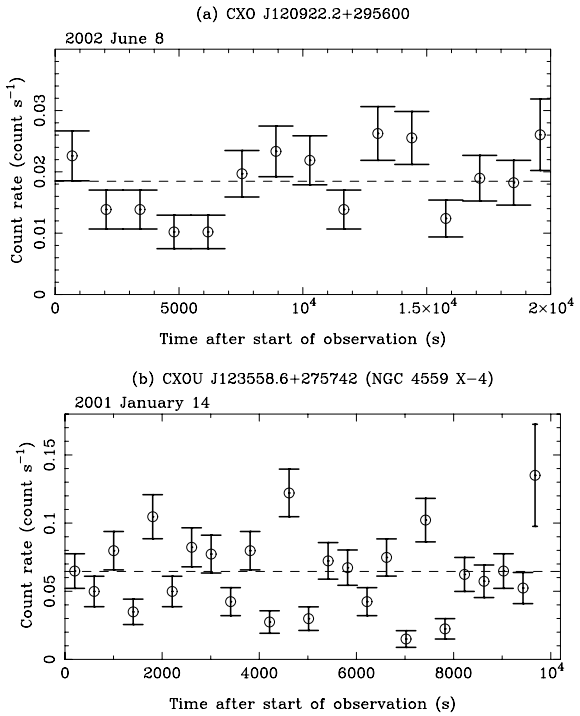

Figure 5. The short-term variability observed in two ULXs. The data in both panels are binned such that at the mean count rate (shown by the dashed line) each temporal bin would contain 25 counts.

both occur when the ULX in question is (on average) at the lower of its two observed X-ray fluxes.

We also performed a Kolmogorov–Smirnov test comparing the cumulative photon arrival times with the expected arrival times, assuming each source flux was invariant with time. This provides a separate indicator of short-term variability, free of any possible gross binning effects, and sensitive to lower amplitude (10–20 per cent) sustained changes in the ULX count rates than the χ^2 test. We performed this test on all eight ULXs. It confirmed that the 2002 June observation of CXOU J120922.2+295600 was variable at >99 per cent probability. Curiously, the 2001 January observation of CXOU J123558.6+275742 was only variable at the ∼90 per cent level according to the Kolmogorov–Smirnov test. Again, none of the other ULXs appeared variable according to this test.

In the 2001 January light curve of CXOU J123558.6+275742 there are four peaks in the X-ray emission, separated by regular intervals of 6–7 bins, during which the X-ray flux is 4–5 times brighter than in the lowest flux bins. This hints at a possible characteristic time-scale for the variability of ∼2500 s for the peaks. It is also noticeable that the light curve behaves similarly between the peaks (this quasi-repetitive behaviour is the likely reason for the lower probability of this source being variable according to the Kolmogorov–Smirnov test). Similar regular variability in the form of quasi-periodic flaring has recently been revealed in three separate observations of an extremely variable ULX in M74, CXOU J013651.1+154547 (Krauss et al. 2003). However, the characteristic time-scales of these variations are somewhat longer, inferred to be at ∼3600–7900 s, and the flares have a larger amplitude, reaching more than an order of magnitude brighter than the quiescent level for this ULX. Claims of actual periodic variations have so far only been made for three ULXs. A period of 7620 ± 500 s was reported for a bright state of the ULX M51 X-7 (Liu et al. 2002b), albeit on the basis of a 15-ks observation. A 7.5-h period was derived for a

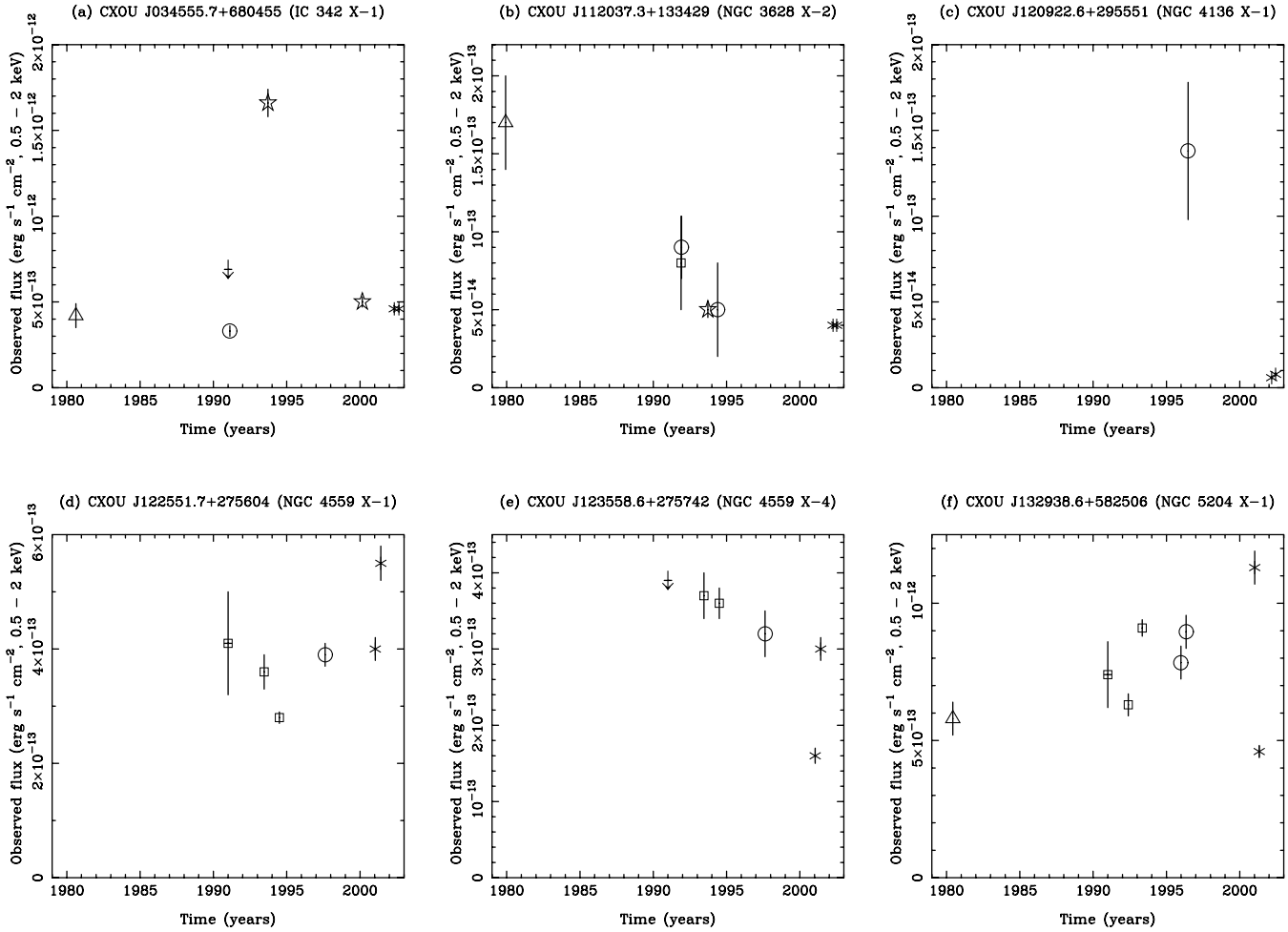

Figure 6. Long-term light curves for six of the ULXs. The data points shown originate from *Einstein* IPC (triangles), *ROSAT* PSPC (squares), *ROSAT* HRI (circles), *ASCA* (stars) and *Chandra* (asterisks) measurements, which have been converted to a 0.5–2 keV flux as described in the text. Each panel is normalized independently to highlight the variability of each ULX.

ULX coincident with the Circinus galaxy (Bauer et al. 2001), though given the proximity of Circinus to the Galactic plane and the similarity of the periodicity to a long-period AM Her system it is possible that this source is a foreground interloper. The only other apparently periodic variations in a ULX were reported by Sugiho et al. (2001) for IC 342 source 3, but these were very small-amplitude (∼5 per cent) and on a time-scale of 30–40 h.

4.3.2 Long-term variability

Six of the eight ULXs have been detected and catalogued in the data from previous X-ray observatories. The long-term variability light curves for these objects are plotted in Fig. 6, using data from the *Einstein*, *ROSAT* and *ASCA* observatories in addition to our new *Chandra* data. Each light curve is plotted in terms of the observed 0.5–2 keV flux of the ULX, with this particular band chosen for its commonality between the missions. The flux is directly measured from our best-fitting spectral models, in the case of the *Chandra* data, or is a flux quoted from previous spectral measurements of the source in question (using *ASCA* and some *ROSAT* PSPC data: see Appendix A for references), or is calculated from the observed count rates or fluxes given in a wider band. In the latter cases, we assume spectral models that are coarse averages of the two *Chandra* observations (e.g. an absorbed power-law continuum model with $\Gamma = 2$ and $N_{\rm H} = 2 \times 10^{20}$ atom cm^{-2} for CXOU J123551.7+275604) and use either PIMMS or XSPEC to normalize the observed count rate into an observed 0.5–2 keV flux. Finally, we correct the *Einstein* and *ASCA* count rates of CXOU J112037.3+133429 for confusion with the two moderately bright sources immediately to its north-northwest (cf. Fig. 1) and we similarly correct the *ROSAT* PSPC data for CXOU J123558.6+275742 for confusion with other sources in proximity to the nucleus of NGC 4559, both on the basis of the *Chandra* observations.

The long-term light curves of the ULXs are obviously very poorly sampled, with between three and eight observations, each typically only a few hours long, covering a baseline from 6 to 23 yr. However, despite the low quality, there does appear to be some variety evident in the behaviour of the different ULXs. Two sources, CXOU J123551.7+275604 and CXOU J132938.6+582506, appear to have varied quite randomly over their observational histories, with a maximum change in their observed flux of little more than a factor of 2. On the other hand, the average flux of CXOU J112037.3+133429 appears to have consistently decayed over 23 yr of observations to ∼25 per cent of the value inferred from the *Einstein* Imaging Proportional Counter (IPC). A possible decay is also observed from CXOU J123558.6+275742, with the exception of a large dip in its

first *Chandra* epoch, which coincides with the epoch of extreme short-term variability in this ULX. A further source whose flux has decayed since its initial detection is CXOU J120922.6+295551, which has faded by a factor ∼20 over the six years between its initial detection in a *ROSAT* HRI image and the current *Chandra* observations. Finally, CXOU J034555.7+680455 appears at around the same 0.5–2 keV flux ($4 \pm 1 \times 10^{-13}$ erg cm^{-2}s^{-1}) in all but one of its observations. The exception is the 1993 September observation in which it displayed a high/soft spectral state, with an average flux four times higher than in other epochs. This may indicate that the high/soft state is rare in this source.

We do not present long-term light curves for the two previously undetected ULXs. The 0.5–2 keV flux of CXOU J120922.2+295600 in the *Chandra* observations was ~ 5–7×10^{-14} erg cm^{-2}s^{-1}: if this flux was the same during the previous *ROSAT* HRI observation of this galaxy, it would have remained undetected (NGC 4136 X-1 ≡ CXOU J120922.6+295551 was a marginal detection at $\sim 1.5 \times 10^{-13}$ erg cm^{-2}s^{-1}). On the other hand, CXOU J123557.8+275807 was observed to have a flux of 3–$\times 10^{-14}$ erg cm^{-2}s^{-1} in the *Chandra* observations, which compares to detection limits of around 1 and 4×10^{-14} erg cm^{-2}s^{-1} in the *ROSAT* PSPC and HRI observations of NGC 4559, respectively. This implies that this ULX is possibly a transient source.

Finally, our *Chandra* observations reveal that two out of the five target ULXs have faded to X-ray luminosities that are below the arbitrary limit of 10^{39} erg s^{-1} that we use to demarcate the ULX population from the 'normal' X-ray source population in nearby galaxies. An important aim for future studies will be to determine how common this behaviour is for ULXs, and in particular to define their duty cycle, allowing us to estimate the true number of potential ULXs in nearby galaxies.

5 DISCUSSION: CLUES TO THE NATURE OF ULXS FROM THEIR BEHAVIOUR?

5.1 Similar behaviour

Are there any general trends revealed in our data that can help cast light on the nature of ULXs? Several similarities across the sample are highlighted by the analysis in the previous sections. They are all spatially consistent with point-like sources, and when their ubiquitous long-term variability (and in some cases extreme short-term variability) is considered it is very likely that their X-ray emission originates in a single X-ray emitting system. The majority of the best-fitting X-ray spectral models show an absorption column well in excess of that along the line-of-sight to each ULX through our own Galaxy. This may be either an additional column through the host galaxy, or perhaps material intrinsic to the ULX itself. The lack of variation in the absorption column where it is constrained by the same physical model at both epochs (cf. Table 4) suggests that it may not originate in the very close proximity of the ULX, although it may still be associated with gas and dust in their immediate environment.

It is likely that the majority of the ULXs are associated with the young stellar populations of the active star formation regions in their host galaxies. The issue of whether this implies that they do not contain an IMBH primary remains controversial. Models for IMBH formation in young, dense stellar clusters (e.g. Ebisuzaki et al. 2001; Portegies Zwart & McMillan 2002) certainly argue that star formation regions could host IMBHs, though the observed displacement between stellar clusters and ULX positions in the Antennae (Zezas et al. 2002) argues that at least in this case many of these ULXs are runaway binaries (i.e. ordinary X-ray binaries kicked out of the stellar clusters by the supernova explosions that formed the compact primary). If alternatively the IMBHs were formed before the current epoch of star formation, for instance as the remnants of the primordial Population III stars (Madau & Rees 2001), it is unlikely that they could accrete sufficient material to appear ULX bright even in the gas-rich environment of star formation regions (cf. Miller & Hamilton 2002), therefore they are reliant upon capturing a secondary star to accrete from. The chances of this occurring could be higher within the dense stellar environments of star-forming regions. However, whatever the origin of the IMBH, King (2004) argues that extremely large underlying populations of these objects are required in order to account for the numbers of ULXs observed in the brightest starburst galaxies such as the Cartwheel galaxy (cf. Gao et al. 2003). This strongly argues that ULXs associated with star formation are, as a class, dominated by ordinary HMXBs that somehow exceed their Eddington limit. In our sample, the likely association of the ULXs with young stellar populations could simply be the extension of the ULX–star formation relationship into lower star formation rate normal spiral galaxies. If so, then it is likely that our objects may also be predominantly HMXBs.

Next, *Chandra* does not detect extreme short-term X-ray variability (on the scale of hundreds of seconds over a baseline of 3–6 h) as a common feature of these ULXs (it is present in only two of 14 observations), implying that in the majority of ULX states either the X-ray emission is reasonably constant, or it varies on much shorter time-scales than we have sampled. The absence of extreme short-term variability, on the basis of *Chandra* observations, has also been noted for many other ULXs in spiral galaxies (cf. Strickland et al. 2001; Roberts et al. 2002). The lack of this behaviour in the majority of ULXs argues strongly against the relativistic beaming model as the dominant emission mechanism for ULXs because presumably this would require a remarkably stable jet to avoid large-amplitude flux variation, as a result of both its narrow beam angle and the strong amplification of any variations via Doppler boosting.

On the other hand, the absence of extreme long-term variability is also interesting, with most of the ULXs seen to vary only by factors of up to ∼4 over periods of up to 20 yr. This suggests that they are all persistent X-ray sources, rather than short duty cycle transients. Interestingly, a comparison with the 18 dynamically confirmed Galactic black hole binaries shows that the only persistent sources over the last ∼30 yr are the three HMXBs (McClintock & Remillard 2003). Furthermore, observations of one of the HMXBs, Cyg X-1, with *RXTE* have shown its flux to vary by no more than a factor of ∼4 over seven years of continuous observations (Pottschmidt et al. 2003). These similarities may be another clue linking ULXs to HMXBs, although whether this is a fair comparison given that the three Galactic HMXB/BH sources are all wind accretors with L_X well below 10^{39} erg s^{-1} is open to debate.

A further trend revealed by the data analysis is that the X-ray spectra of the ULXs are generally better fit by power-law continua than by MCDBB models, with only one out of six ULXs showing a preference for the latter (though we note that in three of the 10 power-law spectra a combination of low signal-to-noise ratio and a low χ^2/d.o.f. value implies that we cannot exclude MCDBB models to a high statistical significance). This appears to contradict previous results, particularly those reported from *ASCA* observations by Makishima et al. (2000), which focused on ULXs well fitted by a MCDBB as possible examples of the high/soft state for accreting 10–100 $M_\odot$ black holes. So if these ULXs are comparable to Galactic sources but are not in the high/soft state, what state are they in? To answer this question we refer to the recent work by McClintock & Remillard (2003), which provides new definitions of the classic

black hole states, with firm observational diagnostics based on the results of more than six years of observations with *RXTE*. However, because we have neither the photon statistics in the *Chandra* data to derive a power density spectrum, nor any information on the X-ray spectrum beyond a maximum of 10 keV, we are reliant solely on the photon indices of the power-law continua to provide a state diagnostic. The two states described by McClintock & Remillard (2003) that provide the best candidates for the power-law-dominated spectra are the low/hard state (which is related to the emission of radio jets) and the steep power-law state (previously known as the very high state), with the distinction in photon indices being that the low/hard state typically has values of $\Gamma \sim 1.5$–2, whereas the steep power-law state has values of $\Gamma > 2.4$. Using this distinction, it is clear that only one source (CXOU J132938.6+582506) has a sufficiently steep power law to be in the latter class ($\Gamma \sim 2.8$–3.0), with all the other sources more consistent with the low/hard state. It is also notable that Galactic black holes in the steep power-law state tend to have a substantial contribution from a MCDBB component with $kT_{\rm in} \sim 1$–2 keV; we do not see any such composite warm MCDBB + power-law continuum spectrum (although the *Chandra* bandpass may not be the optimum choice for recognizing such a spectrum).

This provides an observational argument against the suggestion of Kubota et al. (2002; see also Terashima & Wilson 2004, for further discussion) that the the power-law spectral state of ULXs must be the very high state. Instead, the slopes of the four out of five ULXs best described by power-law spectra suggest that the sources are in the low/hard state. Until recently, this would have suggested that the ULX was accreting at a relatively low fraction (maybe ∼5 per cent) of the Eddington luminosity of the compact object, as black hole states were simplistically assumed to be a function of mass accretion rate (see e.g. Esin, McClintock & Narayan 1997). This would imply black hole masses of 1–2 $\times$ 10^3 $M_\odot$ for these ULXs, i.e. IMBHs. However, it is now clear that the black hole state is not a direct function of mass accretion rate (Homan et al. 2001). This suggests that we cannot rule out observing the low/hard state at or near the Eddington limit for a stellar-mass black hole. However, it is still true that in most known cases the low/hard state occurs well below the Eddington limit, with the one exception being GRS 1915+105 which reaches luminosities $>10^{38}$ erg s^{-1} in this state (McClintock & Remillard 2003). For ULXs to be low/hard state stellar-mass black hole binaries we would obviously have to rely on some means of boosting the apparent luminosity to explain their super-Eddington fluxes, e.g. anisotropic emission. However, observations of the low/hard state in Galactic black holes have suggested that the accretion disc could be truncated at large distances from the black hole ($\gtrsim 100 R_{\rm g}$), which would present a challenge for models in which the anisotropic emission originates in funnelling of the radiation by a geometrically thick inner accretion disc (cf. King 2003, though see McClintock & Remillard 2003 for a discussion of whether the inner disc is truly truncated in the low/hard state). This suggests that the easiest interpretation of this state is that we are observing the low/hard state from accretion on to an IMBH.

The arguments presented above assume that direct analogies to Galactic black hole systems are appropriate for ULXs, when the majority of Galactic black holes spend the majority of their time emitting at far below the 10^{39} erg s^{-1} threshold of ULXs. It is possible then that the hard power-law state we are seeing is actually unique to the very high accretion rates required if ULXs are truly at the extreme high-luminosity end of the stellar-mass black hole population. If this is the case, then super-Eddington ratios (i.e. $L_{\rm X}/L_{\rm Edd}$) of up to 10 are required for the ULXs discussed in this paper: this is consistent with the predictions of Begelman (2002) for true super-Eddington discs and within a factor two of the ratio predicted from simple geometric funnelling by Misra & Sriram (2003). Of course, we cannot rule out accretion on to IMBHs as an explanation for the spectra of any of our sources, but it is worth noting that it is now becoming clear that Galactic black holes do show epochs of apparent super-Eddington emission (McClintock & Remillard 2003). Perhaps the most pertinent example of these Galactic sources is GRS 1915+105, which spends a significant fraction of its time emitting at super-Eddington rates for its ∼14 $M_\odot$ black hole (Done, Wardzinski & Gierlinski 2004) and has been in outburst continually for the past 11 yr. Hence, if viewed by an observer outside our galaxy, GRS 1915+105 could frequently appear as a ULX.

5.2 Contrasting behaviour

A remarkable feature of the analysis in the previous sections is the diversity in the observed properties of the ULXs, with the differences between the objects being more pronounced than any similarities. To obtain a deeper understanding of these objects, we adopt a more complete view than simply considering each characteristic in isolation. We approach this by compiling a summary of their observational characteristics in Table 6.

One immediate curiosity highlighted by Table 6 is that the two sources that display short-term variability appear very different. Whilst both the sources are at the lower of their two observed luminosities when variable, their average X-ray spectra during this epoch contrast greatly, with CXOU J120922.2+295600 displaying a hard power-law continuum ($\Gamma \sim 1.55$) whereas CXOU J123558.6+275742 has a MCDBB form. The short-term variability and power-law spectral form of CXOU J120922.2+295600 may be consistent with its X-ray emission in this state being dominated by a variable, possibly relativistically beamed jet. However, the thermal accretion disc spectrum of CXOU J123558.6+275742 argues against this interpretation. Further studies of short-term variation in ULXs, based on higher signal-to-noise ratio data, have suggested a number of alternative physical mechanisms including rapid variations in the ULX accretion rate (La Parola et al. 2003), magnetic reconnection events in the accretion disc corona (Roberts & Colbert 2003) and an optically thick outflow (Mukai et al. 2003).

A related issue is the long-term variations in the X-ray spectra of these sources revealed by the *Chandra* data. We note, with reference to Table 4, that all the spectra appear to show changes between the two observational epochs. We summarize these changes in Fig. 7 by plotting the best-fitting power-law photon index for each data set against the derived intrinsic 0.5–8 keV X-ray luminosity for that observation. Though Fig. 7 highlights that the 90 per cent confidence intervals for the photon index measurements overlap in almost all cases, consistent with little or no significant change in the photon indices, the best-fitting values do appear to show some level of variation. The data suggest that three of the ULX spectra are softer in a higher luminosity state and three are harder. It has been noted elsewhere (e.g. Kubota et al. 2001; La Parola et al. 2001) that some ULXs undergo a low/hard to high/soft state transition, reminiscent of the behaviour of classic Galactic black hole X-ray binary systems. Other recent observations have highlighted the opposite behaviour, i.e. a high state in which the spectrum is harder, for instance in M51 X-7 (Liu et al. 2002a) and in four out of five ULXs in the Antennae (Fabbiano et al. 2003b), one interpretation being that the accretion disc heats up (and hence spectrally hardens) as the luminosity of the system increases. The equal split between hardening and softening ULXs in our sample suggests that both transitions are common,

Table 6. A summary of the ULX characteristics.

ULX (CXOU J)	Epoch	L_X[a]	Variability		Best-fit spectral model[b]	Environment
			Short-term	Long-term		
034555.7+680455	2002-04-29	4.4(5.9)	No	Hard state + soft flare	PL	Spiral arm
	2002-08-26	4.4(6.4)	No			
112037.3+133429	2002-04-06	0.7(0.8)	No	Steady flux decay	PL	Outer disc
	2002-07-04	0.6(0.7)	No			
120922.2+295600	2002-03-07	2.3(2.6)	No	(N/A)	PL + absorbed MCDBB	Spiral arm
	2002-06-08	1.7(1.9)	**Yes**		→ PL	
120922.6+295551	2002-03-07	0.2(0.2)	No	Large drop	(N/A)	Spiral arm
	2002-06-08	0.2(0.2)	No			
123551.7+275604	2001-01-14	9.8(10.0)	No	Random	PL (+ soft component?)	Faint outer spiral arm
	2001-06-04	11.6(12.5)	No		→ PL + MEKAL	
123557.8+275807	2001-01-14	1.4(1.5)	No	Transient?	(N/A)	Inner disc
	2001-06-04	2.6(2.9)	No			
123558.6+275742	2001-01-14	4.2(4.3)	**Yes**	Gradual fade or random?	MCDBB	Inner disc/bulge
	2001-06-04	8.9(9.1)	No			
132938.6+582506	2001-01-09	5.7(6.9)	No	Random	Soft PL	Inner disc
	2001-05-02	1.8(2.4)	No			

[a]Observed 0.5–8 keV luminosity in units of 10^{39} erg s^{-1}. Figures in parentheses are the intrinsic values. The luminosity of CXOU J120922.6+295551 is converted from the count rate assuming a power-law continuum with $\Gamma = 1.8$ and foreground absorption, whereas the luminosities for CXOU J123557.8+275807 are derived from a rough spectral fit to its second-epoch data (an absorbed MCDBB with $N_H \sim 9 \times 10^{20}$ atom cm^{-2} and $kT_{in} \sim 1.2$ keV).
[b]We use PL as shorthand for a power-law continuum. (N/A) indicates that we did not have sufficient quality data for the analysis.

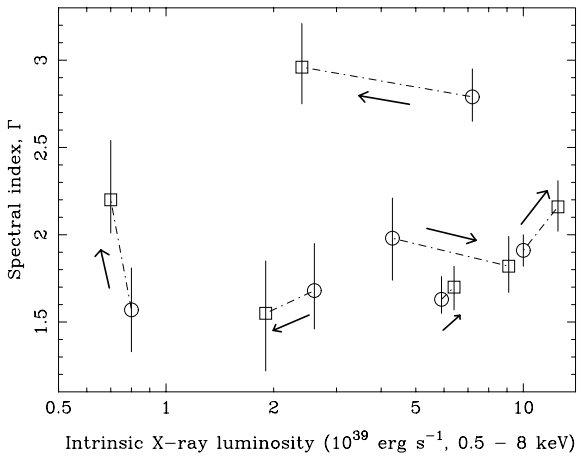

Figure 7. Spectral variability in the ULXs as a function of intrinsic X-ray luminosity. The first-epoch *Chandra* data are indicated by an open circle and the second-epoch data by a square, with the two observations of each source joined by a dot–dashed line. The evolution of the photon index with luminosity is highlighted by the arrows and the errors are the 90 per cent confidence intervals for the spectral parameters.

implying either that the ULX population is heterogeneous, with at least two flavours of accretors behaving differently, or that those sources comprising the bulk of the ULX population are capable of displaying multiple states and modes of transition between those states.

5.3 (Dis)appearing spectral components

Table 6 also highlights a more spectacular flavour of spectral variation: components that appear to be present at one epoch but not during the other. This occurs in two of the ULXs. In CXOU J120922.2+295600 we see a very soft component, fitted by a MCDBB model with $kT_{in} = 0.12$ keV, that is present (though only at 3σ confidence) in the more luminous 2002 March observation but not in 2002 June. A similar soft ($kT < 0.2$ keV) MCDBB component has been reported in other ULX, notably from *XMM–Newton* data for two ULXs in NGC 1313 (Miller et al. 2003a), where it is interpreted as spectroscopic evidence for the cool accretion disc expected to be present around an IMBH. In CXOU J120922.2+295600 this component disappears in the three-month period between observations. This could be analogous with a classic high/soft to low/hard state transition as seen in Galactic black hole X-ray binary candidates, but potentially involving an IMBH system in this case. However, there are other potential explanations. Perhaps the best alternative is that the soft component is originating in an optically thick outflowing photosphere around a black hole X-ray binary, as suggested by Mukai et al. (2003) to account for a highly luminous ultra-soft ULX in M101 (a phenomenon also described as a black hole wind: see King & Pounds 2003; Fabbiano et al. 2003b). Such a component would have a blackbody spectrum with a temperature $kT \sim 0.1$ keV, consistent with the first-epoch observation (cf. Section 4.2.3), and might easily switch off between the two observations of the ULX. However, there are arguments against the soft component originating in a black hole wind, most notably in the case of sources that also have a strong hard power-law continuum component in their spectrum (e.g. M81 X-9: Miller et al. 2003b). In this case the power-law component must originate in shocks outside the photosphere, but in order to have comparable luminosity to the soft component Miller et al. (2003b) argue that the photospheric radius must actually be of the order of the Schwartzschild radius, implying no photosphere for these sources and hence that the soft component must originate in the accretion disc.

The other ULX to show a changing spectral form was CXOU J123551.7+275604. In this case, the spectrum showed a marked softening between the two *Chandra* observations. Earlier, we noted that the additional soft flux present in the second epoch could be modelled in terms of the emergence of soft ($kT = 0.18$ keV) optically thin thermal emission in the ULX spectrum, which was not present five months earlier. Because individual line features are not evident in the raw data, this interpretation is very model-dependent and needs to be checked via future observations. Bearing in mind

these caveats we can, nevertheless, speculate as to how such thermal emission might be produced.

The putative MEKAL component is emitting an incredible $\sim 2.7 \times 10^{39}$ erg s^{-1} of 0.5–8 keV X-ray luminosity if the emission is isotropic. To place this is context, this is an order of magnitude greater than the integrated diffuse luminosity of several small nearby galaxies (cf. Read, Ponman & Strickland 1997). We note that CXOU J123551.7+275604 might not be a unique system: two other ULXs have been reported with possible thermal plasma components, with a similar very soft component reported on the basis of a joint *ROSAT* PSPC/*ASCA* spectral fit of the Holmberg II ULX by Miyaji, Lehmann & Hasinger (2001), and a much hotter and time-variable thermal component detected for a ULX in M51 (Terashima & Wilson 2004).

What processes might produce thin-thermal plasma emission in the X-ray spectrum of a ULX? Miyaji et al. (2001) suggest the presence of one or more supernovae in the immediate environment of the Holmberg II ULX, but we can reject this for CXOU J123551.7+275604 given the rapid appearance of the plasma and the lack of a reported recent supernova at this position. In contrast, Terashima & Wilson (2004) draw an analogy to the X-ray spectrum of some HMXBs in eclipse, which are dominated by emission-lines that originate in photoionization of the stellar wind by the hard X-ray emission of the accreting primary (e.g. Cyg X-3; cf. Liedahl & Paerels 1996). However, we cannot be observing thermal emission as a result of a reduction in contrast with the direct emission from the ULX because we measure a higher overall flux in the second-epoch observation when the plasma component is present. In any event, the plasma component we measure appears far too soft, at 0.18 keV, to be directly analogous to the photoionized stellar wind in sources such as Cyg X-3, which are typically identified by strong emission lines at energies well above 1 keV.

The emission measure of the plasma is $n_{\rm e}^2 V = 2.9 \times 10^{63}$ cm^{-3}, where $n_{\rm e}$ is the electron density in atom cm^{-3} and V is the volume of the material. Because the plasma is optically thin, it must satisfy the limit $n_{\rm e} r < 1/\sigma_{\rm T}$, where r is the path-length through the plasma and $\sigma_{\rm T}$ is the Thomson scattering cross-section. Combining these two estimates gives $r_{\rm min} \approx 3 \times 10^9$ km, implying that the plasma occupies a region far larger than the black hole accretion disc. However, as we argue above, it is probably too soft to be a photoionized stellar wind, which leaves the alternative possibility that it is a collisionally ionized system. This could arise if an outflow from the ULX (perhaps in the form of a relativistic jet)[5] impacts upon a cloud of material relatively close to the ULX.

We further speculate that this scenario might occur if the secondary star in the system is an evolved high-mass star because these are known to eject discrete shells of material, for example, with luminous blue variable (LBV) stars thought to lose up to $\times 10^{-3}$ M$_\odot$ yr^{-1} in such discrete outburst events (van der Sluys & Lamers 2003 and references therein). For the derived value of $r_{\rm min}$, we calculate an electron density $n_{\rm e,max} \approx 4.9 \times 10^9$ cm^{-3} and hence a mass of 4.8×10^{-4} M$_\odot$ for the plasma, well within the ejection masses quoted above. To energize this mass of material to a temperature of $kT = 0.18$ keV requires an energy input of $E = 3N_{\rm e}kT$, where $N_{\rm e}$ is the total number of electrons in the plasma, hence, a total of at least $\sim 4.8 \times 10^{44}$ erg is required. In the 141 days between the observations, this would require an average mechanical energy input from the outflow of at least $\sim 4 \times 10^{37}$ erg s^{-1}. We note that this energy input could be easily achievable by relativistic jets: for example, the W50 radio bubble surrounding SS 433 probably originates in inflation by the mildly relativistic jets of SS 433, with an average mechanical energy input from the jets of 3×10^{39} erg s^{-1} (Dubner et al. 1998). Hence, this scenario appears physically plausible.

Finally, we note that if the collisionally excited material does originate in the ejection of matter from an evolved high-mass star, then this scenario is consistent with the suggestion of King et al. (2001) that ULXs are fed by thermal-time-scale mass transfer from an evolved secondary star in a HMXB. However, it is not clear whether this system could be an ordinary HMXB containing a stellar-mass black hole in accordance with the King et al. (2001) model, as Cropper et al. (2004) conclude that its observational characteristics point towards it containing an IMBH.

Clearly future monitoring of the behaviour of CXOU J123551.7+275604 is required to resolve many of the uncertainties as to its nature, and in particular to investigate whether outflow/stellar material collision events occur in reality.

6 CONCLUSIONS

In this paper we have studied dual-epoch observations of five nearby ULXs obtained with the *Chandra* ACIS-S detector. These have revealed heterogeneity in the observed properties of ULXs, from the characteristics of individual sources varying between the observation epochs, to a wide range of observed X-ray properties across the sample. The main outcomes of our analysis are as follows.

(i) We detect all five target ULXs, though two have faded to luminosities below 10^{39} erg s^{-1}, plus we find three additional ULXs within the regions of the galaxies that we observe.

(ii) The ULXs are all likely to be associated with the young stellar populations residing in and around the star-forming regions of their host galaxies. This is consistent with the discovery of large ULX populations in starburst galaxies, extending the ULX–young stellar population link to normal spiral galaxies. We estimate that no more than two out of the eight ULXs originate in older stellar populations on the basis of the ULXs per unit optical luminosity measured in elliptical galaxies by Colbert & Ptak (2002).

(iii) All the ULXs are point-like at the 0.5-arcsec on-axis *Chandra* resolution.

(iv) We derive the spectral parameters for six ULXs in both observational epochs, finding that the majority (five) are best fitted by a power-law continuum rather than a MCDBB model, contrary to some previous reports for ULXs (e.g. Makishima et al. 2000). Two of the five best fitted by power laws require an additional, very soft spectral component in at least one observation.

(v) Extreme short-term variability (on a time-scale of hundreds of seconds) is observed in only two ULXs and in these sources it is only seen in one of two observations. However, all the ULXs with archival data are variable by factors of a 2–4, over time-scales of years.

(vi) The lack of short-term variability, unless it occurs on time-scales much less than our temporal sampling, may indicate that the X-ray emission of ULXs as a class is not dominated by relativistically beamed jets.

(vii) By utilizing the new black hole state diagnostics of McClintock & Remillard (2003), we see that four out of the five power-law-dominated spectra have photon indices consistent with the low/hard state. This challenges the recent assertions that power-law-dominated spectra in ULXs originate in the very high state.

[5] It is quite reasonable for a ULX to possess a relativistic jet regardless of whether or not it dominates the X-ray emission. By way of analogy, Galactic black hole systems such as GRS 1915+105 (i.e. microquasars) certainly do possess relativistic jets that do not dominate their X-ray emission.

However, if this truly is the low/hard state it could pose problems for interpretations of ULXs involving anisotropic stellar-mass black holes, and the simplest explanation would be that we are seeing a low/hard state from accretion on to an IMBH. The alternative is that we might be observing a state unique to the very high accretion rates required for stellar-mass black hole models.

(viii) We find that equal numbers of ULXs (three apiece) show spectral hardening and softening with increasing luminosity. This indicates either an underlying physical heterogeneity in the ULX population or, perhaps, that the bulk of the ULX population is composed of sources that can behave in both ways.

(ix) The X-ray spectrum of CXOU J123551.7+275604 is particularly interesting in that it is possible that a very soft and luminous MEKAL component appears in the five months between the two observations. We speculate that this plasma (if real) originates in the impact of an outflow (possibly relativistic jets) from the ULX on material in its close vicinity. One possible source of this material could be in discrete mass-ejection events from an evolved high-mass secondary star. The presence of an evolved high-mass companion star is consistent with the scenario suggested by King et al. (2001), where many ULXs are ordinary HMXBs with an evolved high-mass secondary, though conversely this ULX is a very good candidate for an IMBH.

The properties outlined above portray ULXs as a class with very heterogeneous properties. Whilst some trends are emerging, such as the likely relation between many ULXs and young stellar populations, the lack of observable short-term variability and a preference for power-law continuum spectra, none of these provides conclusive observational evidence to distinguish between the competing physical models. It could be that much of the confusion is because ULXs are a physically heterogeneous class, including both stellar-mass black holes, many of which could be in HMXBs, and IMBHs. Therefore, perhaps, the question we should be addressing is: to what degree are the ULX populations heterogeneous? An answer to this question is reliant upon future large samples of high-quality X-ray data, plus detailed multi-wavelength follow-up, to study these objects in much greater detail. It appears that we are still at the beginning of the long road towards understanding these extraordinary X-ray sources.

ACKNOWLEDGMENTS

The authors would like to thank the anonymous referee for their comments, which have greatly improved the interpretation of our results. The authors would also like to thank Paulina Lira for an initial discussion on targets for this programme. TPR gratefully acknowledges support from PPARC. This research has made use of the NASA/IPAC Extragalactic Database (NED), which is operated by the Jet Propulsion Laboratory, California Institute of Technology, under contract with the National Aeronautics and Space Administration. This research has also made use of data obtained from the Leicester Database and Archive Service at the Department of Physics and Astronomy, Leicester University, UK. The second Digitized Sky Survey was produced by the Space Telescope Science Institute, under Contract No. NAS 5-26555 with the National Aeronautics and Space Administration.

REFERENCES

Angelini L., Loewenstein M., Mushotzky R. F., 2001, ApJ, 557, L35
Bauer F. E., Brandt W. N., Sambruna R. M., Chartas G., Garmire G., Kaspi S., Netzer H., 2001, AJ, 122, 182
Baumgardt H., Hut P., Makino J., McMillan S., Portegies Zwart S., 2003, ApJ, 582, L21
Begelman M. C., 2002, ApJ, 568, L97
Bregman J. N., Glassgold A. E., 1982, ApJ, 263, 564
Bregman J. N., Pildis R., 1992, ApJ, 398, L107
Bregman J. N., Cox C. V., Tomisaka K., 1993, ApJ, 415, L79
Colbert E. J. M., Mushotzky R. F., 1999, ApJ, 519, 89
Colbert E. J. M., Ptak A. F., 2002, ApJS, 143, 25
Cropper M., Soria R., Mushotzky R. F., Wu K., Markwardt C. B., Pakull M., 2004, MNRAS, in press
Crosthwaite L. P., Turner J. L., Ho P. T. P., 2000, AJ, 119, 1720
Dahlem M., Heckman T. M., Fabbiano G., 1995, ApJ, 442, L49
Dahlem M., Heckman T. M., Fabbiano G., Lehnert M. D., Gilmore D., 1996, ApJ, 461, 724
Davis J. E., 2001, ApJ, 562, 575
de Vaucouleurs G., de Vaucouleurs A., Corwin H. G.Jr, Buta R. J., Paturel G., Fouqué P., 1991, Third reference catalogue of bright galaxies. Springer, New York
Done C., Wardzinski G., Gierlinski M., 2004, MNRAS, submitted (astro-ph/0308536)
Dubner G. M., Holdaway M., Goss W. M., Mirabel I. F., 1998, AJ, 116, 1842
Ebisuzaki T. et al., 2001, ApJ, 562, L19
Esin A. A., McClintock J. E., Narayan R., 1997, ApJ, 489, 865
Fabbiano G., Trinchieri G., 1987, ApJ, 315, 46
Fabbiano G., Kim D.-W., Trinchieri G., 1992, ApJS, 80, 531
Fabbiano G., Zezas A., Murray S. S., 2001, ApJ, 554, 1035
Fabbiano G., Zezas A., King A. R., Ponman T. J., Rots A., Schweizer F., 2003a, ApJ, 584, L5
Fabbiano G., King A. R., Zezas A., Ponman T. J., Rots A., Schweizer F., 2003b, ApJ, 591, 843
Falco E. et al., 1999, PASP, 111, 438
Gao Y., Wang Q. D., Appleton P. N., Lucas R. A., 2003, ApJ, 596, L171
Gebhardt K., Rich R. M., Ho L. C., 2002, ApJ, 578, L41
Georganopoulos M., Aharonian F. A., Kirk J. G., 2002, A&A, 388, L25
Gerssen J., van der Marel R. P., Gebhardt K., Guhathakurta P., Peterson R. C., Pryor C., 2002, AJ, 124, 3270
Goad M. R., Roberts T. P., Knigge C., Lira P., 2002, MNRAS, 335, L67
Ho L. C., Filippenko A. V., Sargent W. L. W., 1997, ApJS, 112, 315
Homan J., Wijnands R., van der Klis M., Belloni T., van Paradijs J., Klein-Wolt M., Fender R., Mendez M., 2001, ApJS, 132, 377
Immler S., Pietsch W., Aschenbach B., 1998, A&A, 331, 601
Irwin J. A., Athey A. E., Bregman J. N., 2003, ApJ, 587, 356
Kaaret P., Prestwich A., Zezas A., Murray S., Kim D.-W., Kilgard R., Schlegel E., Ward M., 2001, MNRAS, 321, L29
Kaaret P., Corbel S., Prestwich A. H., Zezas A., 2003, Sci, 299, 365
King A., 2002, MNRAS, 335, L13
King A., 2003, in Lewin W. H. G., van der Klis M., eds, Compact Stellar X-ray Sources, in press (astro-ph/0301118)
King A., 2004, MNRAS, 347, L18
King A., Pounds K. A., 2003, MNRAS, 345, 657
King A., Davies M. B., Ward M. J., Fabbiano G., Elvis M., 2001, ApJ, 552, L109
Körding E., Falcke H., Markoff S., 2002, A&A, 382, L13
Krauss M., Kilgard R., Garcia M., Roberts T. P., Prestwich A., 2003, ApJ, submitted
Kubota A., Mizuno T., Makishima K., Fukazawa Y., Kotoku J., Ohnishi T., Tashiro M., 2001, ApJ, 547, L119
Kubota A., Done C., Makishima K., 2002, MNRAS, 337, L11
La Parola V., Peres G., Fabbiano G., Kim D. W., Bocchino F., 2001, ApJ, 556, 47
La Parola V., Damiani F., Fabbiano G., Peres G., 2003, ApJ, 583, 758
Liedahl D. A., Paerels F., 1996, ApJ, 468, L33
Lira P., Lawrence A., Johnson R. A., 2000, MNRAS, 319, 17
Lira P., Ward M. J., Zezas A., Alonso-Herrero A., Ueno S., 2002, MNRAS, 330, 259
Liu J.-F., Bregman J. N., Seitzer P., 2002a, ApJ, 580, L31
Liu J.-F., Bregman J. N., Irwin J., Seitzer P., 2002b, ApJ, 581, L93

McClintock J. E., Remillard R. A., 2003, in Lewin W. H. G., van der Klis M., eds, in Compact Stellar X-ray Sources, in press (astro-ph/0306213)
Madau P., Rees M. J., 2001, ApJ, 551, L27
Makishima K. et al., 2000, ApJ, 535, 632
Mason K. O. et al., 2000, MNRAS, 311, 456
Miller J. M., Fabbiano G., Miller M. C., Fabian A. C., 2003a, ApJ, 585, L40
Miller J. M., Fabian A. C., Miller M. C., 2003b, ApJ, submitted (astro-ph/0310617)
Miller M. C., Hamilton D. P., 2002, MNRAS, 330, 232
Mirabel I. F., Rodriguez L. F., 1999, ARA&A, 37, 409
Mirabel I. F., Mignani R., Rodrigues I., Combi J. A., Rodriguez L. F., Guglielmetti F., 2002, A&A, 395, 595
Misra R., Sriram K., 2003, ApJ, 584, 981
Mitsuda K. et al., 1984, PASJ, 36, 741
Miyaji T., Lehmann I., Hasinger G., 2001, AJ, 121, 3041
Mizuno T., Kubota A., Makishima K., 2001, ApJ, 554, 1282
Mukai K., Pence W. D., Snowden S. L., Kuntz K. D., 2003, ApJ, 582, 184
Okada K., Dotani T., Makishima K., Mitsida K., Mihara T., 1998, PASJ, 50, 25
Portegies Zwart S. F., McMillan S. L. W., 2002, ApJ, 576, 899
Pottschmidt K. et al., 2003, A&A, 407, 1039
Read A. M., Ponman T. J., Strickland D. K., 1997, MNRAS, 286, 626
Reynolds C. S., Loan A. J., Fabian A. C., Makishima K., Brandt W. N., Mizuno T., 1997, MNRAS, 286, 349
Roberts T. P., Colbert E. J. M., 2003, MNRAS, 341, L49
Roberts T. P., Warwick R. S., 2000, MNRAS, 315, 98 (RW2000)
Roberts T. P., Goad M. R., Ward M. J., Warwick R. S., O'Brien P. T., Lira P., Hands A. D. P., 2001, MNRAS, 325, L7
Roberts T. P., Warwick R. S., Ward M. J., Murray S. S., 2002, MNRAS, 337, 677
Roberts T. P., Goad M. R., Ward M. J., Warwick R. S., 2003, MNRAS, 342, 709
Stark A., Gammie C. F., Wilson R. W., Bally J., Linke R. A., Heiles C., Hurwitz M., 1992, ApJS, 79, 77
Strickland D. K., Colbert E. J. M, Heckman T. M., Weaver K. A., Dahlem M., Stevens I. R., 2001, ApJ, 560, 707
Sugiho M., Kotoku J., Makishima K., Kubota A., Mizuno T., Fukazawa Y., Tashiro M., 2001, ApJ, 561, L73
Terashima Y., Wilson A., 2004, ApJ, 601, 735
Tully R. B., 1988, Nearby Galaxies Catalog. Cambridge Univ. Press, Cambridge
van der Marel R. P., Gerssen J., Guhathakurta P., Peterson R. C., Gebhardt K., Pryor C., 2002, AJ, 124, 3255
van der Sluys M. V., Lamers H. J. G. L. M., 2003, A&A, 398, 181
Veron-Cetty M.-P., Veron P., 2000, ESO Sci. Rep., 19, 1
Voges W. et al., 1999, A&A, 349, 389
Vogler A., Pietsch W., Bertoldi F., 1997, A&A, 318, 768
Wu H., Xue S. J., Xia X. Y., Deng Z. G., Mao S., 2002, ApJ, 576, 738
Yaqoob T., Serlemitsos P. J., Ptak A., Mushotzky R., Kunieda H., Terashima Y., 1995, ApJ, 455, 508
Zezas A., Fabbiano G., 2002, ApJ, 577, 726
Zezas A., Fabbiano G., Rots A. H., Murray S. S., 2002, ApJ, 577, 710
Zezas A., Ward M. J., Murray S. S., 2003, ApJ, 594, L31

APPENDIX A: PREVIOUS OBSERVATIONS OF THE ULXs

A1 IC 342 X-1 (CXOU J034555.7+680455)

This ULX was first detected in an *Einstein* IPC observation of IC 342, with a 0.2–4 keV X-ray luminosity of 3×10^{39} erg s^{-1} (Fabbiano & Trinchieri 1987). A subsequent *ROSAT* HRI observation detected IC 342 X-1 in a similarly luminous state (Bregman, Cox & Tomisaka 1993; RW2000) . An early *ASCA* observation showed IC 342 X-1 to be in a very luminous, highly variable state in which its average 0.5–10 keV luminosity surpassed 10^{40} erg s^{-1} and it displayed large-amplitude variability on ∼1000 s time-scales (Okada et al. 1998). In this state its X-ray spectrum was well fitted by the multicolour disc blackbody model describing an accretion disc around a black hole in a high/soft state (Makishima et al. 2000). However, a follow-up observation obtained late in the *ASCA* mission showed the ULX to have dimmed to a luminosity of 6×10^{39} erg s^{-1} and undergone a spectral transition to a low/hard state, similar to the behaviour observed in many Galactic and Magellanic black hole X-ray binary systems (Kubota et al. 2001; Mizuno et al. 2001). However, the low/hard spectral state has recently been reinterpreted as a high/anomalous state where the X-ray spectrum is described by a strongly Comptonized optically thick accretion disc, as observed in many Galactic black hole X-ray binaries experiencing a high mass accretion rate (Kubota et al. 2002). Finally, recent William Herschel Telescope integral field unit observations have revealed that this ULX lies at the centre of a large nebula, probably a supernova remnant shell (Roberts et al. 2003, and references therein). The inferred initial energy input to the supernova remnant is consistent with a hypernova event and highly excited (O III) emission-line regions on the inner edge of the shell suggest that the ULX is photoionizing its inner regions to produce an X-ray ionized nebula.

A2 NGC 3628 X-2 (CXOU J112037.3+133429)

This source was first detected as point source two in a 1979 December *Einstein* IPC image of NGC 3628, as reported by Bregman & Glassgold (1982), where it was observed to lie at the eastern end of the edge-on galaxy disc. They derived a 0.3–2.9 keV luminosity of 2.1×10^{39} erg s^{-1} for NGC 3628 X-2, corrected to our assumed a distance of 7.7 Mpc (this correction is assumed for all the following luminosities). However, the reprocessed IPC data contour map presented by Fabbiano, Kim & Trinchieri (1992) suggests, in retrospect, that this flux may be an upper limit as a result of confusion with two X-ray sources since resolved to the north of X-2.[6] It was also detected in three separate *ROSAT* observations, once with the PSPC and twice with the HRI, as reported in Dahlem, Heckman & Fabbiano (1995) and Dahlem et al. (1996). In particular, the 1991 November PSPC observation provides a measurement of its X-ray luminosity in the 0.1–2 keV band of 0.6×10^{39} erg s^{-1}, several times lower than the *Einstein* value. This apparent variability is supported by the *ROSAT* HRI images, which demonstrate that the count rate of NGC 3628 X-2 drops substantially between 1991 December and 1994 May. NGC 3628 X-2 was also detected in a 1993 December *ASCA* observation (Yaqoob et al. 1995). Its *ASCA* SIS spectrum is well fitted with a simple power-law continuum model, with $\Gamma \sim 2.4$ and an absorption column of $N_{\rm H} \sim 7 \times 10^{21}$ atom cm^{-2}, well in excess of the foreground Galactic column. This model implies luminosities of 0.7 and 1.7×10^{39} erg s^{-1} in the 0.5–2 and 2–10 keV bands, respectively, consistent with the *ROSAT* PSPC measurement in the soft X-ray regime, though this must again be regarded as an upper limit as a result of the likelihood of confusion with other sources in the wide *ASCA* beam. Yaqoob et al. (1995) comment that the X-ray spectrum of NGC 3628 X-2 is consistent with either a low-mass X-ray binary or a very young supernova remnant, noting that if it is an accreting source then it is substantially super-Eddington for a 1 $M_\odot$ object. Finally, NGC 3628 X-2 was not covered in the

[6] These sources are now identified as the QSO J112041.7+133552 (Veron-Cetty & Veron 2000) and a narrow-emission-line galaxy RIXOS 259-7 (Mason et al. 2000).

previous *Chandra* ACIS-S observation of NGC 3628 discussed by Strickland et al. (2001), as their observation was aligned along the minor axis of the galaxy.

A3 NGC 4136 X-1 (CXOU J120922.6+295551)

The first and, previous to this work, only detection of this ULX was made by Lira et al. (2000), who obtained a luminosity of 2.5×10^{39} erg s^{-1} (corrected to a distance of 9.7 Mpc) from a *ROSAT* HRI observation of NGC 4136. They note that its position is coincident with a diffuse blue optical counterpart, which may be emission knots in the spiral arms of the galaxy.

A4 NGC 4559 X-1 (CXOU J123551.7+275604) and X-4 (CXOU J123558.6+275742)

NGC 4559 X-1 was first detected in the *ROSAT* All-Sky Survey bright source catalogue as 1RXS J123551.6+275555 (Voges et al. 1999). It was identified with the outer edge of the galactic disc of NGC 4559 by Vogler, Pietsch & Bertoldi (1997), who present a detailed analysis of the X-ray properties of this source based on a *ROSAT* PSPC pointed observation. In their work, they refer to this source as NGC 4559 X-7. The PSPC profile of the source is point-like and no significant X-ray variability was detected from it during the observation. Its spectrum is well fitted by either a power-law continuum ($\Gamma \sim 3$) or thermal bremsstrahlung model ($kT \sim 0.8$ keV), both showing absorption $N_{\rm H} \sim 1$–2×10^{21} atom cm^{-2}, well in excess of the foreground Galactic column. The observed (0.1–2.4 keV) luminosity of 2×10^{39} erg s^{-1} converts to an impressive intrinsic luminosity of 1.5×10^{40} erg s^{-1} using the thermal bremsstrahlung model. The PSPC position is coincident with a group of emission knots in a faint outer spiral arm of the galaxy, which Vogler et al. (1997) identify as likely H II regions. It is, however, too bright to be the integrated X-ray emission of ordinary X-ray binaries and supernova remnants associated with the H II region. They conjecture that this source is most likely a supernova remnant buried in a dense cloud of interstellar material, though they do not rule out either a black hole accreting binary system or mini-AGN from a merging dwarf galaxy, as alternative identifications. This source was also detected, with a similar high X-ray luminosity, in a *ROSAT* HRI observation (RW2000).

Unlike NGC 4559 X-1, NGC 4559 X-4 was not detected in the *ROSAT* All-Sky Survey bright source catalogue. However, in the *ROSAT* PSPC observation reported by Vogler et al. (1997) (who list this ULX as NGC 4559 X-10) it was brighter than X-1. It is located near, but not at, the centre of the galaxy. It appears as an extended source in the PSPC observation, with approximately 20 per cent of its flux emanating from between 20 and 50 arcsec from the source centroid, which may be a diffuse component, or confusion with other point sources (with our *Chandra* data suggesting the latter). The X-ray spectrum is well fitted by either a power-law continuum or thermal bremsstrahlung emission, albeit spectrally harder in each case than for X-1 ($\Gamma \sim 2.0$ or $kT \sim 2.1$ keV, respectively), with a measured absorption column of $N_{\rm H} \sim 10^{21}$ atom cm^{-2}. This gave an observed (intrinsic) luminosity of $7(12) \times 10^{39}$ erg s^{-1}. Vogler et al. (1997) suggest that X-10 is the superposition of several point sources, though they cannot rule out the contribution of an AGN towards the observed flux. This source is again also detected in the *ROSAT* HRI survey of RW2000, offset from the nucleus of NGC 4559 by 13 arcsec.

A5 NGC 5204 X-1 (CXOU J132938.6+582506)

This ULX was first detected in an *Einstein* IPC observation, with a 0.2–4 keV X-ray luminosity of $\sim 2.6 \times 10^{39}$ erg s^{-1} (Fabbiano et al. 1992). It also appeared in the *ROSAT* All-Sky Survey bright source catalogue with a count rate of 7.5×10^{-2}counts^{-1}. Later *ROSAT* HRI pointed observations revealed NGC 5204 X-1 to lie $\sim$20 arcsec to the east of the nucleus of NGC 5204 (Colbert & Mushotzky (1999); RW2000; Lira et al. (2000)). This ULX was revealed to have a point-like optical counterpart with a blue continuum spectrum in a William Herschel Telescope integral field observation (Roberts et al. 2001), suggestive of the presence of several O-stars. A more detailed study using archival *HST* data resolved the ULX into three possible counterparts, all of which are consistent with young ($<$10 Myr old) compact stellar clusters in NGC 5204, suggesting that this ULX may be a high-mass X-ray binary system (Goad et al. 2002).

This paper has been typeset from a TEX/LATEX file prepared by the author.